SHORT TERM CONTRACT FOR THE BIOLOGICAL STUDIES (ICCAT GBYP 05/2021) OF THE ATLANTIC-WIDE RESEARCH PROGRAMME FOR BLUEFIN TUNA (GBYP Phase 11)

Final Report
for:

ICCAT

Scientific coordinator:

Dra. Igaratza Fraile (AZTI-Member of Basque Research & Technology Alliance)

Pasaia, May 31th, 2022

This project is co-funded by the European Union

PARTNERS:

Fundación AZTI-AZTI Fundazioa

IFREMER

Fisheries Research Institute, Japan Fisheries Research and Education Agency

Instituto Español de Oceanografía - CSIC

Texas A&M University

GMIT

Universidad de Cádiz

National Oceanic and Atmospheric Administration

Fisheries and Oceans of Canada

SUBCONTRACTORS and COLLABORATORS:

	Institute of Marine Research
	Instituto Português do Mar e da Atmosfera
	Institut National de la Recherche en Halieutique
	The University of Arizona
	Centre National de la Recherche Scientifique
	Sgiker (Euskal Herriko Unibertsitatea)
	Thermofisher
	CBBA

INDEX:

EXECUTIVE SUMMARY:

The main objective of this project is to enhance knowledge about Atlantic bluefin tuna (ABFT) population structure and mixing, but also to focus on age dynamics.

During Phase 11, the Consortium sampled a total of 452 Atlantic bluefin tuna (129 YOY, 1 juvenile fish, 47 medium sized fish and 275 large fish) from different regions (140 from the Strait of Gibraltar, 41 from Portugal, 34 from the Canary Islands, 180 from Norway, 22 from the Central North Atlantic, 34 from the South of Spain and 1 from the Bay of Biscay). In total, 1067 biological samples (309 otolith samples, 307 fin spines and 451 genetic samples) were collected by the Consortium and incorporated into the tissue bank. The Consortium also received samples from other ICCAT contracts with tagging teams and farm operators. In total, the Consortium handled 3198 biological samples (1046 otolith samples, 995 fin spines and 1157 genetic samples) from 1189 individuals. All these samples have been catalogued and stored together with the biological tissue bank, which is undergoing a restructuring process to revise and standardize all the information gathered over the last 10 years of the project.

On genetic analyses we have improved the 96 SNP traceability panel by replacing the least informative markers with the newly selected 10 SNPs including 7 best performing SNPs for traceability and 3 genetic markers for sex identification. We have further clarified the population structure of ABFT by re-analyzing previously generated RAD-seq data to obtain a Copy Number Variant (CNVs) dataset, by analyzing Whole Genome Sequencing data of 25 ABFT and 2 *Thunnus alalunga* individuals and by analyzing > 700 samples genotyped with the SNP array. The combined study of the mixing dynamics at feeding aggregates based on genetic markers and otolith microchemistry confirmed assignment mismatch between methods, identifying samples with contradicting genetic and geographic origin. Genetic markers for sex identification integrated in both the 96 SNP traceability panel and the SNP array allowed to correctly assign sex at high classification rates. The potential epigenetic approaches for ageing in ABFT samples has been evaluated.

Regarding otolith microchemistry, new carbon ($\delta^{13}C$) and oxygen ($\delta^{18}O$) stable isotope analyses were carried out in 119 otoliths of Atlantic bluefin tuna captured in the Central North Atlantic, Morocco and Norwegian Sea, to determine their nursery area. Otolith $\delta^{13}C$ and $\delta^{18}O$ values measured in otolith cores indicated that these samples were dominated by eastern origin individuals. These results combined with previous analyses suggest that mixing of the two populations occurs at variable rate in the western North Atlantic, but Mediterranean bluefin tuna may be the principal contributor to the Northeast Atlantic fisheries. Additionally, otolith $\delta^{18}O$ measurements using high-precision secondary ion mass spectrometry (SIMS) and isotope ratio mass spectrometry (IRMS) were cross-calibrated. IRMS measurements of $\delta^{18}O$ were linearly related to $\delta^{18}O$ from the same otolith portion, obtained using SIMS (IRMS $\delta^{18}O = 0.36*(SIMS\ \delta^{18}O) +0.25$; R2 =0.63). This regression can be used to convert SIMS measurements to their equivalent IRMS measurements, allowing for comparison across studies and integration of information from both techniques. Ten archival tags were purchased and planning for future deployment in a tuna farm in Malta commenced. Otolith $\delta^{18}O$ profiles from tagged fish for the period of captivity can be related to internal and external temperature profiles from the tags to parameterize the relationship between $\delta^{18}O$ and water chemistry, and to examine the influence of internal physiology.

Controversies remain regarding the periodicity, or seasonality, of otolith growth band formation which directly influences a correct age determination of Atlantic bluefin tuna using otoliths. Thereby, the aim of the work on ageing carried out under this contract was to apply marginal increment analysis (MIA) and marginal edge analysis to determine the timing of band deposition. The index of completion (MIA) was also analyzed using General Additive Models (GAMs) to evaluate the importance of variables such as month, age/size, reading criteria, light type and reader. Results indicated that the opaque bands begin to form in July and continue to form up until October. The translucent band starts to form in November and peaks in May and June, with the highest percentage of wide translucent bands. GAM model indicated that the opaque band would finish forming in November.

.

From the end of the year and the beginning of the following year there is minimal marginal edge growth, and this is when the translucent band begins to form and reaches its maximum development in June. MIA and marginal edge analyses have evidenced that the annulus in the Atlantic Bluefin tuna otolith start to be formed in November. This would mean to delay the date of the current July 1st adjustment criterion to November 30. The change in the date of the otolith fitting criterion allows for a better outline of the strong 2003-year class. Age results based on otolith counts have been updated accordingly in the ICCAT catalogue.

Recently, ABFT larvae were found in the Bay of Biscay (Rodriguez et al. 2021) demonstrating that ABFT can spawn in this area. During the current phase, additional plankton samples were collected and analysed under the microscope in search of ABFT larvae. We found no evidence of ABFT larvae in the Bay of Biscay region, in agreement with previous findings suggesting that the bluefin spawning in the Bay of Biscay could be sporadic phenomenon.

Finally, ABFT larvae from surveys conducted in the Balearic Sea spawning ground were sorted and identified for potential close-kin analyses. In total, 2880 individuals from 30 samples collected during 2019 were identified. Bluefin tuna larvae were found in 18 out of the 30 samples analysed. In addition, stages of larval development were identified (i.e., yolk sac, preflexion, flexion, or postflexion). The sorted individuals were preserved in 100% ethanol in different 4 ml jars and kept in the freezer for a perfect conservation.

Overall, most of the objectives of the project were met. These analyses continue to provide relevant information for a better understanding of the biology of Atlantic bluefin tuna, which in turn improves the stock assessment and management advice of this valuable species.

1. CONTEXT

On July 9th 2021, the Consortium coordinated by AZTI- Member of Basque Research & Technology Alliance, and formed by partners AZTI, IFREMER, Fisheries Research Institute (Japan Fisheries Research and Education Agency), Instituto Español de Oceanografía del Consejo Superior de Investigaciones Científicas (IEO/CSIC), Texas A&M University (TAMU), Galway-Mayo Institute of Technology (GMIT), Universidad de Cádiz (UCA), National Oceanic and Atmospheric Administration (NOAA), Fisheries and Oceans of Canada (DFO), with subcontracted parties IPMA, IMR and INRH for the sampling task, presented a proposal to the call for tenders on biological and genetic sampling and analysis of Atlantic bluefin tuna launched by GBYP program (ICCAT-GBYP 05/2021).

This proposal was awarded and the final contract between ICCAT and the Consortium represented by Fundación AZTI-AZTI Fundazioa was signed on July 13th 2021.

According to the terms of the contract, a Final Report (Deliverable nº 5) needed to be submitted to ICCAT by the 31st of May 2022. The present report was prepared in response to such requirement.

2. SAMPLING

Task Leader: Iraide Artetxe-Arrate (AZTI)

Participants:

AZTI: Inma Martin, Naiara Serrano, Ainhoa Arevalo, Goretti Garcia, Maite Cuesta, Igaratza Fraile, Naiara Rodriguez-Ezpeleta, Natalia Diaz, Iñaki Mendibil, Patricia Lastra, Iker Zudaire

UCA: Jose Luis Varela, Antonio Medina, Esther Asensio, Edurne Blanco, Aurelio Ortega

NRIFSF: Yohei Tsukahara

IEO: Enrique Rodriguez Marín, Rosa Delgado de Molina

INRH: Noureddine Abbid

IMR: Ørjan Sørensen, Leif Nøttestad

IPMA: Pedro Lino, Ruben Lechuga-Muñoz, Rui Coelho

2.1 Introduction

The sampling conducted under this project follows a specific design, aimed primarily at contributing to knowledge on population structure and mixing. As such, the sampling conducted under this project is independent from other routine sampling activities for fisheries and fishery resources monitoring (e.g., the Data Collection Framework). The sampling protocols, together with instructions, have been distributed within the Consortium as well as to ICCAT, so that they are distributed to other institutions conducting biological sampling (e.g. as part of tagging activities, Regional Observer Programs, farms, etc.).

2.2 Sampling accomplished

The agreed sampling for Phase 11 has been accomplished for the North Sea, Northeast Atlantic, Strait of Gibraltar and Canary Islands in the East Atlantic (Table 2.1). In total 997 samples from 510 ABFT individuals have been achieved by the Consortium, consisting of 274 otoliths, 306 dorsal fin spines and 417 muscle tissue for genetics (Table 2.2).

Table 2.1: a) Individuals sampled within the Consortium, in each area and per each age stratum. Last column represents the percentage (%) obtained over the agreed sampling target for Phase 11, green when the target was accomplished, red when target couldn't be accomplished. b) Total number of individuals sampled (including those of the Consortium plus the ones sampled under other contracts and stored by the Consortium).

a)		Size-class sampled				Responsible (Sampler)	Target	%
		Age 0	Juvenile	Medium	Large			
		<3 Kg	3-25 Kg	26-100 Kg	>100 Kg			
North Sea	Norway	0	1	0	179	AZTI (IMR)	100	180
Central North Atl.	Central North Atl.	0	0	1	21	FRI	300	7
Northeast Atlantic	Bay of Biscay	0	0	1	0	AZTI	0	-
	Portugal (Algarve)	0	0	0	41	AZTI (IPMA)	30	137
	Canary Islands	0	0	0	34	IEO	30	113
Strait of Gibraltar	Gibraltar	95	0	45	0	UCA	50	280
Western Med.	South Spain	34	0	0	0	UCA	0	-
TOTAL nº		**129**	**1**	**46**	**276**		**510**	**89%**

b)		Size-class sampled				Responsible (Sampler)	Total
		Age 0	Juvenile	Medium	Large		
		<3 Kg	3-25 Kg	26-101 Kg	>100 Kg		
North Sea	Norway	0	1	0	179	AZTI (IMR)	180
Central North Atl.	Central North Atl.	0	0	1	21	FRI	22
Northeast Atlantic	Bay of Biscay	0	0	1	0	AZTI	1
	Portugal (Algarve)	0	0	0	41	AZTI (IPMA)	41
	Canary Islands	0	0	0	34	IEO	34
Strait of Gibraltar	Gibraltar	95	0	45	0	UCA	140
Western Med.	South Spain	34	0	0	0	UCA	34
	Balearic Islands	0	0	4	335	TAXON	339
	Tyrrhenian Sea	0	0	10	41	ABTL	51
Central Med.	Malta	0	0	24	323	ABTL/ROP	347
TOTAL nº		**129**	**1**	**84**	**975**		**1189**

The IMR has provided samples of 179 large and 1 juvenile individuals. The large individuals consisted of 168 specimens from two purse seine landings from M/S Spjæringen and, in addition, two individuals which entered Atlantic salmon fish farms and nine individuals from the GBYP satellite tagging project at IMR. The juvenile fish was caught on rod and reel in Varangerfjord at ~70°N. In total, 123 otoliths, 171 spines and 180 muscle tissue for genetics were collected. One of the reasons for the reduced otolith amount (still above the target, i.e., 100 otoliths) in comparison with the other tissues, is that most of the ABFT are sold with heads on, it was not possible to extract the otoliths from many of the individuals. Besides, in 2021 purse seine vessels have landed earlier than previous seasons and have thus not kept the fish for cooling as long as before. This has resulted in a narrower time window for the technicians at IMR to get on the landing site in time and thus be able to conduct their various biological samplings. This might be partly explained by the low market prices, and also to the fact that several fishing vessels with quota have not prioritized ABFT fishing in this area during 2021 because of the Brexit an, as well by the conflict with mackerel fishing in the Northeast Atlantic; Norwegian purse seiners, which have spent much more time fishing mackerel when this is more dispersed in Norwegian waters, dropping their fishing for ABFT this year. It is uncertain whether the situation may remain the same for next year.

In the Portuguese coast off Algarve, 41 large ABFT have been sampled from a tuna trap by IPMA staff onboard a factory ship during the tuna harvest season. Tuna heads were used in the manufacturing process, and therefore otolith extraction was not possible. Therefore, the received samples consisted of 41 spines and 41 muscle tissue for genetics.

In the Strait of Gibraltar, 140 individuals have been sampled by UCA, consisting of 95 YOY and 45 medium sized ABFT, caught in traps from Ceuta, artisanal handline fisheries operating in the strait and coastal waters of Málaga by trolling gear. All tissue types were well above the agreed target, in total 95 otolith (all from YOY), 94 spines (all from YOY) and 140 (95 YOY + 45 medium sized) muscle samples for genetic have been achieved. Besides, UCA also provided 34 YOY samples from the South of Spain derived from trolling fisheries operating in the Alboran Sea (Table 2.2).

In the East Atlantic-West African Coast, 34 large individuals have been sampled by the IEO around Canary Islands. No spines were taken from these individuals; therefore, the

obtained tissue samples consist of 34 otoliths and 34 muscle tissue for genetics. Samples have been received by the end of May, but the biological data from these individuals are still missing, and is expected that they willbe received by the next few weeks. Unfortunately, INRH communicated that Moroccan samples will not be available for sampling until September 2022. Thus, although agreed in the initial plan, this subcontracted activity was agreed to be removed from the original sampling plan in the *Proposal to amend the "Short-Term contract for Biological Studies (ICCAT GBYP 05/2021) of the Atlantic-Wide Research Programme for Bluefin Tuna (GBYP Phase 11)*".

In the Central North Atlantic, observer activities on board Japanese longliners have been limited due to the pandemic, and for that reason it was not possible to collect the targeted (300) individuals by FRI (former NRIFSF). As an alternative, 21 large individuals and a medium individual with known catch information were sampled in the market, from which 22 otoliths and 22 muscle tissue for genetics were obtained. This implies that only the 7% of the target has been achieved in this area, being also the reason why the overall objective has not been reached (i.e., 82% of the target achieved), even though in the rest of the areas it has far been exceeded (>100%) (Table 2.1a).

Altogether (considering the samples collected by the Consortium and those that arrived from other contracts), the total number of individuals sampled in this phase have been 1192, consisting of 129 YOY, 1 juvenile, 83 medium and 979 large sized ABFT (Table 2.1b). Overall, the Consortium handled 3202 biological samples; 1049 otoliths, 996 dorsal fin spines and 1157 muscle or fin tissues for genetics (Table 2.3). All these samples have been cataloged and stored together within the biological tissue bank, where nowadays, in total, samples from 23782 individuals are available for analyses: otoliths from 10952 individuals, spines from 7886 individuals, gonads from 2044 individuals and genetic tissue samples from 23395 individuals (Table 2.4)

Table 2.2. Detailed number of otoliths, fin spines and muscle tissue samples achieved in the framework of the Consortium.

Grand Area	Area	Sampler	Otolith	Spine	Muscle/Fin	*Total*
North Sea	Norway	IMR	123	171	180	474
Central North Atlantic	Central North Atlantic	FRI	22	0	22	44
Northeast Atlantic	Bay of Biscay	AZTI	1	1	0	2
	Portugal (Algarve)	IPMA	0	41	41	82
East Atlantic-West African Coast	Canary Islands	IEO	34	0	34	68
Strait of Gibraltar	Gibraltar	UCA	95	94	140	329
Western Mediterranean	South Spain	UCA	34	0	34	68
Total			**309**	**307**	**451**	**1067**

Table 2.3. Detailed number of otoliths, fin spines and muscle tissue samples achieved in Phase 11 (including those of the Consortium plus the ones taken under other contracts and stored by the Consortium).

Grand Area	Area	Sampler	Otolith	Spine	Muscle/Fin	*Total*
North Sea	Norway	IMR	123	171	180	474
Central North Atlantic	Central North Atlantic	FRI	22	0	22	44
Northeast Atlantic	Bay of Biscay	AZTI	1	1	0	2
	Portugal (Algarve)	IPMA	0	41	41	82
East Atlantic-West African Coast	Canary Islands	IEO	34	0	34	68
Strait of Gibraltar	Gibraltar	UCA	95	94	140	329
Western Mediterranean	South Spain	UCA	34	0	34	68
	Balearic Islands	TAXON	343	330	330	1003
		ROP	0	0	9	9
	Tyrrhenian Sea	ABTL	51	50	42	143
Central Mediterranean	Malta	ABTL	343	308	321	972
		ROP	0	0	4	4
Total			**1046**	**995**	**1157**	**3198**

Table 2.4. Detailed number of otoliths, fin spines, gonads and muscle tissue samples storage in the tissue bank and available for analyses.

Grand Area	Otoliths	Spines	Gonads	Muscle/Fin
Central Mediterranean	3447	1406	51	4804
Central North Atlantic	593	2	0	2977
East Atlantic	153	25	0	705
Eastern Mediterranean	797	860	7	1691
Gibraltar Strait	371	175	0	902
Gulf of Mexico	0	0	0	207
North East Atlantic	491	704	0	1628
North Sea	146	604	0	1265
North West Atlantic	0	0	0	360
Western Mediterranean	4954	4110	1986	8856
Total	10952	7886	2044	23395

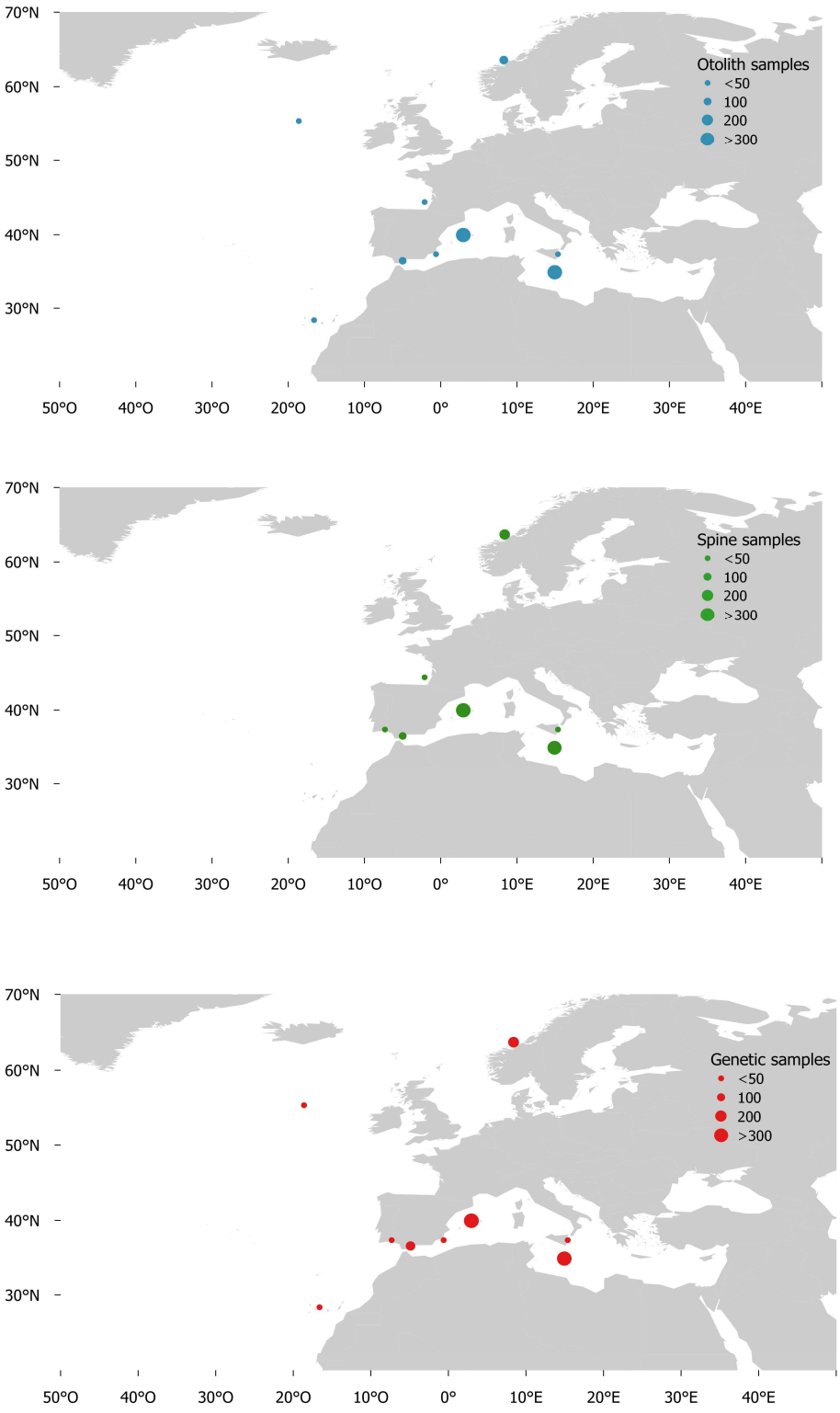

Figure 2.1: Total number of otoliths (blue), fin spines (green) and genetic samples (red) collected under all GBYP contracts in Phase 11. Samples are aggregated by main area.

3. MAINTENANCE OF THE ICCAT GBYP TISSUE BANK

Task Leader:

Igaratza Fraile and Iraide Artetxe-Arrate (AZTI)

Participants:

AZTI: Ainhoa Orbe, David Alvarez

ICCAT`s Secretariat

Tissue bank and related information system is undergoing a restructuring process with the ultimate goal of creating a database with an interface that is easily manageable for any user who requires it. The database that has been in use to date was created at the beginning of the project, an Excel table of > 25MB which has been transformed and expanded as GBPY evolved, but that is becoming difficult to manage due to the magnitude that the project has achieved.

During this phase, the existing excel has been cleaned and restructured. So far, performed actions included:

1) The review of the parameters used for conversions between different types of sizes, weights, and conversion factors between them. These formulas have been standardized, and information has been included as to which type of formula has been used in each case.

2) Revision and adaptation of the date information given. All dates have been provided in a standard format (dd/mm/yyyy).

3) Standardization of the classifications given for different biological parameters such as Sex and Reproductive stage, and estimated age.

4) Location information is being revised individually, and corrected when required (e.g., mismatches between latitude and longitude and the Area given). For this purpose, the original databases sent by each partner at the time are being revised.

5) Results regarding genetic origin, microchemistry origin, otolith annual counts and spine annual counts have been included. Besides, examples of different types of original data files have sent to ICCAT´s secretariat to contribute to the ongoing design and development of a global ICCAT database on biological data. These examples include both consolidated (age estimates based on otoliths, age estimates based on spines, stable isotopes 1 year template and stable isotopes 3-month template) and unconsolidated results (raw RAD-seq data, otolith 2D trace element maps, otolith shape analyses, otolith SIMS analyses and otolith transect analyses).

The revision, standardization, and cleaning of all the available information to date is being continuously updated, while new information from the current phase has been included in the spreadsheet (Appendix 2). Steps are being taken to bridge the gap between the biological information of each bluefin tuna and the results obtained in the different analytical tasks. In addition, the sampling protocol and sampling sheet have been updated to meet the current working needs, as the previous one had become a bit outdated. It is expected that it can be distributed within the Consortium as well as to ICCAT soon.

4. GENETICS

Task Leader:

Naiara Rodriguez-Ezpeleta (AZTI)

Participants:

AZTI: Natalia Diaz-Arce, Iñaki Mendibil, Natalia Gutierrez, Iker Zudaire, Haritz Arrizabalaga

4.1 Introduction

Previous research had shown that population structure of Atlantic Bluefin tuna (ABFT) is more complex than the previous assumption of two reproductively isolated populations (Gulf of Mexico and Mediterranean Sea) that mix for feeding in the Atlantic, and that, contrastingly, individuals from the Gulf of Mexico and Mediterranean Sea interbreed. Yet, the frequency in which this interbreeding occurs in still unknown. Understanding the phenomena driving existing genetic differentiation between the Gulf of Mexico and Mediterranean populations despite this interbreeding is paramount for developing appropriate management and conservation measures.

During previous phases, genotyping of Atlantic bluefin tuna individuals based on thousands of informative Single Nucleotide Polymorphisms (SNPs) for genetic profile study, focused mainly on reference individuals from the Gulf of Mexico and Mediterranean Sea spawning grounds, was carried out. Along the last years the study of the genetic profile of samples from different feeding aggregates using a cost-effective SNP array (developed in GBYP phase 10), especially in combination with microchemistry data, has allowed for an improved understanding of Atlantic bluefin tuna dynamics.

This SNP array also includes markers for sex assignment as well as markers for detecting mitochondrial introgression and adaptation. The analysis of these type of markers allowed to further understand the potential role of strong local adaptation on the maintenance of genetic differentiation between Atlantic bluefin tuna populations.

Previous work has shown that using genetic information instead of location information for origin assignment baselines improves assignment rates (see GBYP Phase 9) but that

even including an enlarged baseline with more reference samples from the Gulf of Mexico (see GBYP Phase 10), unassigned and incorrectly assigned samples remain. This could be due to the initial 96 SNPs selected (see GBYP Phase 5), which didn't consider the information that later became available (see GBYP Phases 5-10). The modification of the SNP combination included in the panel by removing the least informative ones and adding a few more informative ones has allowed for the improvement of the available 96 SNP panel, which includes now 3 new promising markers for sex identification adapted from (Suda et al. 2019).

In addition, the samples and genetic data collected so far could be used for future Close Kin Mark Recapture (CKMR) studies, for which new information, such as the potential of epigenetic methods for ageing (Mayne et al. 2021), was gathered. In addition, the validity and operationality of the molecular sex determination method) was evaluated (Suda et al. 2019; Chiba et al. 2021.

Thus, to further understand the phenomena driving genetic differentiation despite gene flow, the mixing and interbreeding dynamics of ABFT, and to evaluate the potential epigenetic approaches for ageing in ABFT samples, five main tasks have been carried out:

Task 1 has consisted of new data generation by extracting new DNA samples of > 600 individuals, the improvement of the 96 SNP traceability panel by replacing the least informative markers by 10 newly selected ones (including 3 genetic markers for sex identification), and the genotyping of 564 and 384 individuals using the improved 96 SNP traceability panel and the SNP array respectively.

Task 2 has consisted of the analysis of ABFT population structure using three different datasets: a Copy Number Variants (CNVs) dataset obtained from the re-analysis of the available RAD-seq data, the analysis of Whole Genome Sequencing data produced for 25 and 2 ABFT and *Thunnus alalunga* individuals respectively, and the analysis of > 700 samples genotyped using the SNP array.

Task 3 has consisted of the analysis of genetic variability at different feeding aggregates by combining genetic information based on different types of markers with otolith microchemistry data.

Task 4 has consisted of the evaluation of the performance of the genetic sex markers included in the SNP array and the 96 SNP traceability panel for sex identification using genetic tools.

Task 5 has consisted of an evaluation of the potential of epigenetic approaches for ageing ABFT samples.

4.2 Material and methods

4.2.1 DNA extraction

DNA of 624 new samples was extracted. This number is less than that originally planned (1000) because we aimed at maximizing the number of individuals for which otolith microchemistry data are available, from which some of them had DNA extracted from previous GBYP Phases, and because some individuals that had already been genotyped using different techniques were included for method comparison. DNA was extracted using the Wizard® Genomic DNA Purification kit (Promega, WI, USA) following manufacturer´s instructions for "Isolating Genomic DNA from Tissue Culture Cells and Animal Tissue". The starting material was approximately 20 mg of tissue or whole larvae and after extraction all samples were suspended in equal volumes of Milli-Q water. DNA quantity (ng/µl) was evaluated on the Qubit® 2.0 Fluorometer (Life Technologies) and DNA integrity was assessed by electrophoresis.

4.2.2 SNP Array genotyping and analysis

In total, 384 DNA samples (107 newly extracted) were genotyped with the 10,000 SNP array developed in Phase 10, including 359 individuals captured at different feeding aggregate locations for which otolith microchemistry was available (Table 4.1). Another 25 samples already genotyped using RAD-seq in previous GBYP phases were included for result comparison.

Table 4.1. *Number of samples from feeding aggregates captured at each location genotyped using the SNP Array.*

Location	N

Bay of Biscay	65
Central Atlantic	83
Strait of Gibraltar	57
Western Atlantic	70
Canary Islands	43
Norwegian sea	41
TOTAL	359

The newly obtained genotypes were analyzed together with those obtained in Phase 10, totalling767 samples (383 genotyped in Phase 10 and 384 from Phase 11), to homogenize genotype filtering criteria. Genotypes were analyzed and assessed using Axiom Analysis Suite specific software setting default parameters. Individuals and genetic markers which did not met minimum quality standards were removed from the dataset following the Axiom Analysis Best Practices Workflow. Mitochondrial markers, as well as markers designed for genetic sex identification are expected to deviate from the standard genotype distribution, as mitochondrial markers should in theory be homozygous and genetic sex markers should contain only two of the possible three allele combinations. Thus, genotypes of these markers were assigned based on visual observation of cluster plots. Replicate individuals from the RAD-seq dataset and abnormally long/short fin samples analyzed in GBYP Phase 10 were excluded from further analysis and four different datasets were generated using PLINK (Purcell et al. 2007) including the different types of markers genotyped with the SNP array: i) neutral, ii) adaptive, iii) sex and iv) mitochondrial markers. Genetic relatedness of all individuals was assessed based on neutral markers building a genetic relatedness matrix using the software GCTA (Yang et al. 2011) and one individual of each pair of relatives, or all individuals in case of groups of related individuals, were removed from the dataset for further analysis. Datasets containing neutral and adaptive SNPs were exported to structure format using PGDSpider (Lischer, Excoffier 2011). Principal Component Analysis (PCA) was performed using the *adegenet* R package (Jombart 2008) and individual proportions of ancestral populations (assuming two ancestral populations, K=2) were estimated using ADMIXTURE (Alexander, Novembre, Lange 2009). From sex and mitochondrial markers datasets, markers and individuals with missing rates higher than 0.1 and 0.3 respectively were excluded from further analysis. The dataset containing mitochondrial markers was used to identify individuals showing the albacore like mitochondrial haplotype based on four successfully genotyped mitochondrial introgression markers. The dataset containing

sex marker genotypes was used for evaluation of their suitability for genetic sex identification.

4.2.3 Improvement of the Fluidigm SNP panel for origin traceability.

The genotyping of an increased number of samples since the design of the 96 SNPs traceability panel in GBYP Phase 5 allows the selection of traceability markers using a more complete reference dataset representative of the reference populations. We merged RAD-seq and the SNP array (SNP array genotypes generated in Phase 11 were still not available and therefore not considered here) generated genotypes. Those SNPs showing replicability between both techniques lower than 96% based on the 25 replicate samples genotyped with both methods, were removed. Larvae, Young of the Year and sexually mature adults captured in the Mediterranean Sea or the Gulf of Mexico were considered as reference for the Mediterranean and the Gulf of Mexico genetic profiles respectively, except for those adult individuals captured at the Gulf of Mexico identified as Mediterranean-like in GBYP Phase 9, which were excluded. The final dataset included 240 and 299 reference individuals for the Mediterranean Sea and Gulf of Mexico spawning areas respectively and a total of 6,825 SNPs. AllSNPs were ranked based on their informativeness for assignment of individuals to each of the two genetic origins using TRES (Kavakiotis et al. 2015) and the best 19 SNPs were selected. Flanking sequences for each SNP were retrieved for probe design using the script developed in GBYP Phase 5 (https://github.com/rodriguez-ezpeleta/ABFT_popgentrace) and adapted in GBYP Phase 10 for the probe designing for the SNP array.

The probe sequences for the best 19 SNPs for genetic origin assignment and for 5 markers for genetic sex adapted from Suda et al. (2019) that had been developed in GBYP phase 10 for the SNP array were sent for evaluation for probe designing. In total 16 new SNPs for genetic origin and genetic sex assignment for which probe designing for the Fluidigm platform was possible were selected for incorporation in the 96 SNP panel. To select the 16 least informative markers for origin assignment the 96 SNPs from the original 96 SNP panel from (Rodríguez-Ezpeleta et al. 2019) were ranked according to their informativeness for assignment using TRES (Kavakiotis et al. 2015), using the baseline including all the reference individuals for which genotypes of the 96 SNP panel were available (the "enlarged" baseline generated in GBYP Phase 10 report). The least informative 16 SNPs were excluded from the panel.

All samples were genotyped on the BiomarkTM HD platform using Flex Six™ and 96.96 Dynamic Array IFCs, and the resulting data was analyzed with the Fluidigm Genotyping Analysis Software. To test the performance of the new 16 SNP probes, a first round of 94 individuals were genotyped, including 30 individuals which had already been genotyped using RAD-seq or the SNP array. The results were exported and analyzed using PLINK (Purcell et al. 2007). Bad performing SNPs (missing data rates over 0.1 or more than 2 mismatches between SNP panel and RAD-seq or SNP array derived genotypes among the 30 replicate samples) were removed from the panel and substituted by the best performing among the 16 least informative SNPs that had been excluded in the previous step. After readjusting the final SNP combination, 470 individuals were genotyped using the final 96 SNP panel. Obtained results will be splitted into two genotype tables, containing sex identification and genetic origin markers respectively, excluding individuals and SNPs with missing rate higher than 0.1 respectively.

From the total of 564 genotyped samples 50 individuals for which gonad tissue samples were available for histological visualization for sex identification were included. The other 514 included 30 samples which had already been genotyped with RAD-seq or the SNP array for replicability testing, and samples captured at different feeding aggregates and for which otolith microchemistry data was available. There was no available tissue from any individual with recovered electronic tags, and therefore it was no possible to genotype any sample of this type.

4.2.4 Population structure of Atlantic bluefin tuna based on Copy Number Variants inferred from RAD-seq data

The study of Copy Number Variants (CNVs) has been probed to add information on population structure for some species which was not reflected on SNPs. We applied the method developed in Dorant et al. (2020), which allowed to infer CNVs from the available RAD-seq dataset generated in previous GBYP phases. The method accounts for distortion from the expectation on the haplotype proportions at each genotyped SNP, to identify those derived from CNVs, allowing to compare read coverage between samples after read count normalization. We followed the filtering criteria and the cut-off threshold values for CNV detection proposed in Dorant et al. (2020). Once candidates for CNVs were identified, these were extracted from the total dataset and the read count table was exported to a VCF format file. Counts were normalized using the edge R package. Inter-individual

distances were estimated from normalized read counts and used to perform Principal Component Analysis (PCA) using the function *prcomp* from stats R package.

4.2.5 Analysis of whole genome sequencing data

Whole genome sequencing data was generated for two samples of *Thunnus alalunga* and 25 Atlantic bluefin tuna. Reads were filtered by sequencing quality, aligned against the most complete available reference genome of *Thunnus orientalis* (Suda et al. 2019). Aligned individuals reads were filtered by mapping quality and Variants were called using GATK software (Van der Auwera, O'Connor 2020). Haplotype calling is running on a server.

4.2.6 Assessing the potential of epigenetics to age Atlantic Bluefin Tuna samples

For assessing the potential of epigenetic approaches for ageing Atlantic Bluefin tuna samples, a review of the available methodology and of the cases where the approach was used was performed (the outcomes of this task are presented as a stand-alone document in Annex I).

4.3 Results and discussion

4.3.1 The 96 SNP panel for origin traceability was successfully improved

From the 24 candidate tested probes, three and one corresponding respectively to genetic-origin and sex-assignment diagnostic SNPs were not designable due to GC content outside specifications or to the presence of SNPs within the flanking regions. A first round of 94 samples was genotyped with a 96 SNP panel which included the 80 most informative SNPs from the previous panel and 16 new ones: the four designable probes for sex assignment, and the best 12 from the 15 new designable ones for genetic origin. After analysis of these first results, 5 SNPs for genetic origin assignment were excluded from the final panel due to high missing rates and/or low replicability. Besides, one of the included genetic markers was no informative and was also excluded from the final SNP panel. In substitution, the best 6 performing SNPs among the 16 SNPs that had been excluded in the first round were re-included in the panel (Table 4.2). The final panel thus contained 86 SNPs already considered in the original panel and 10 new ones: 3 for sex

determination and 7 for genetic origin assignment. All the 7 newly incorporated SNPs for genetic origin assignment showed better informativeness for assignment scores than the excluded ones (Table 4.2).

Table 4.2. *List of genetic markers that were removed and newly included in the SNP traceability panel. The type of marker is indicated if selected for genetic origin traceability or genetic sex identification. Informativeness for assignment scores estimated by TRES software and used for SNP ranking are indicated.*

Marker	Change	Type	Informativeness for Assignment Score
GBYP-RAD_21	Removed	Genetic Origin	0.00013
GBYP-RAD_54	Removed	Genetic Origin	0.00008
GBYP-RAD_200	Removed	Genetic Origin	0.00008
GBYP-RAD_204	Removed	Genetic Origin	0.00007
GBYP-RAD_142	Removed	Genetic Origin	0.00006
GBYP-RAD_132	Removed	Genetic Origin	0.00006
GBYP-RAD_199	Removed	Genetic Origin	0.00002
GBYP-RAD_84	Removed	Genetic Origin	0.00002
GBYP-RAD_222	Removed	Genetic Origin	0.00001
GBYP-RAD_127	Removed	Genetic Origin	0
Sex_IB	Included	Sex Identification	-
Sex_IIA	Included	Sex Identification	-
Sex_III	Included	Sex Identification	-
GBYP-11-RAD-304	Included	Genetic Origin	0.13729
GBYP-11-RAD-318	Included	Genetic Origin	0.07628
GBYP-11-RAD-305	Included	Genetic Origin	0.05223
GBYP-11-RAD-307	Included	Genetic Origin	0.04977
GBYP-11-RAD-308	Included	Genetic Origin	0.04927
GBYP-11-RAD-311	Included	Genetic Origin	0.04406
GBYP-11-RAD-306	Included	Genetic Origin	0.03808

The remaining 470 individuals have been sent for genotyping with the final SNP panel and we are waiting for the genotyping results to perform genetic origin assignment of the samples and integration with origin assignment based on otolith microchemistry and genetic sex data to understand Atlantic bluefin tuna migration movements.

4.3.2 Population structure of Atlantic bluefin tuna based on neutral markers

Analysis of genetic relatedness between individuals genotyped using the SNP array revealed the presence of 22 kin pairs, one trio and one quartet. Expectedly, all these relations except from three pairs involved larvae captured within the Gulf of Mexico and a time period of two days. The other three detected kin relationships involved pairs of adult individuals of similar birth years estimated based on otolith ring counts. In total, 27 samples were excluded from further analysis: one from each pair, two from the trio and three from the quartet. These results prove that the SNP array is suitable for detecting kin pairs and thus for future studies on Atlantic bluefin tuna CKMR.

The analysis of the 640 samples and 7,719 neutral SNPs genotyped using the SNP array kept after data filtering showed that, as suggested by previous results, all the samples from the different feeding aggregate locations fit within the two ancestral genetic profiles representative of the Mediterranean Sea and Gulf of Mexico spawning grounds (Figure 4.1). In general, most individuals captured within the Eastern stock show Mediterranean-like genetic profiles, while genetic origin of the individuals captured within the Western stock are more variable, including Mediterranean-like and admixed profiles.

There were no otolith microchemistry data available for Gulf of Mexico nor for West Atlantic samples, but in the other locations Gulf of Mexico and Mediterranean Sea otolith microchemistry profiles were found. Particularly, in the Canary Islands and the Central West Atlantic, most of the genetically Gulf of Mexico-like individuals showed a Gulf of Mexico otolith origin. Still, in these regions there were genetically Mediterranean-like and intermediate individuals with Gulf of Mexico otolith origin, suggesting that genetically Mediterranean-like individuals could be originated out from the Mediterranean Sea.

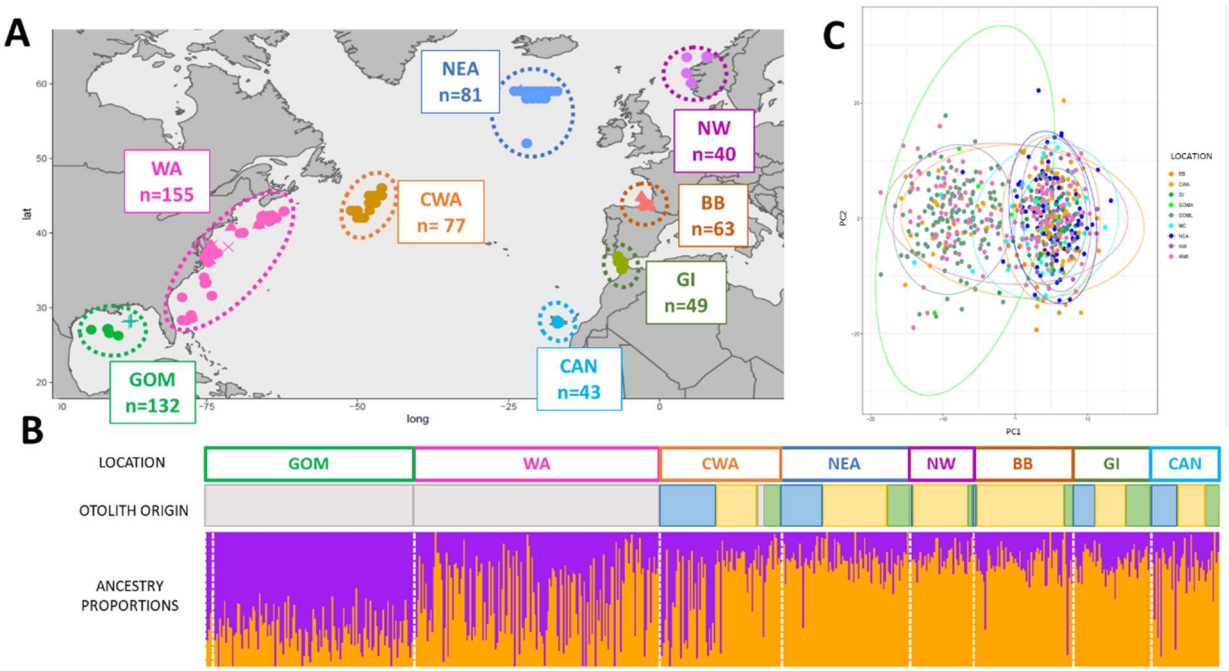

Figure 4.1. *Genetic origin of the 640 samples genotyped using the SNP array captured at different feeding aggregates and within the Gulf of Mexico based on neutral markers. A. Catch locations of genotyped samples, where each dot represents one individual and the different colors represent different locations (GOM=Gulf of Mexico, WA= West Atlantic, CWA= Central West Atlantic, NEA= North East Atlantic, NW = Norwegian Sea, BB = Bay of Biscay, GI=Strait of Gibraltar, CAN= Canary Islands). Crosses within the GOM represent larvae samples. B. Individual proportions from each of the two ancestral populations of Atlantic bluefin tuna. Catch locations are indicated, and origin assigned based on otolith microchemistry (otolith origin) is indicated for each sample in blue is assigned to the Gulf of Mexico), yellow when assigned to the Mediterranean Sea) and green if unassigned. Samples for which otolith origin was not available are represented in grey. C. PCA performed using the same dataset shows that genetic diversity of all samples is explained by distribution of samples in two main clusters and several intermediate individuals.*

4.3.3 Population structure and mixing dynamics at feeding aggregates based on outlier and mitochondrial markers

Analysis of genetic variability based on outlier markers clustered samples in three different groups, in agreement with what it was observed in GBYP Phase 10 (Figure 4.2). The explanation for this three-clustering pattern is that outlier markers aggregate within a genomic region under high linkage disequilibrium, which means that haplotypes have a high probability of being inherited together.

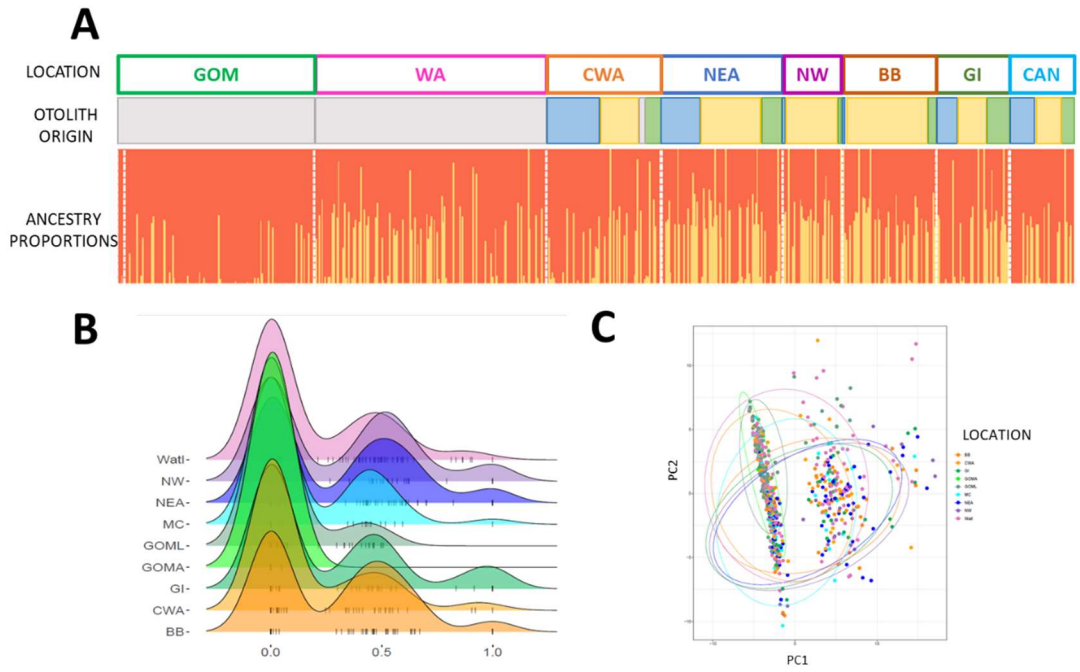

Figure 4.2. *Genetic diversity of the 640 samples genotyped using the SNP array captured at different feeding aggregates and within the Gulf of Mexico based on adaptive markers. A. Individual ancestry proportions assuming two ancestral populations based on outlier markers. Catch locations are indicated as GOM=Gulf of Mexico, WA= West Atlantic, CWA= Central West Atlantic, NEA= Northeast Atlantic, NW = Norwegian Sea, BB = Bay of Biscay, GI=Strait of Gibraltar, CAN= Canary Islands. Origin assigned based on otolith microchemistry (otolith origin) is indicated for each sample in blue is assigned to the Gulf of Mexico), yellow when assigned to the Mediterranean Sea) and green if unassigned. Samples for which otolith origin was not available are represented in grey. B. Frequency distribution of individual ancestry values represented in A for each sampled location. C. PCA performed using the same dataset shows that genetic diversity of all samples is explained by distribution of samples in three main clusters along the first Principal Component.*

The frequency of individuals belonging to each of these three clusters, hereafter group 1, group 2 and group 3 for the most common to the rarest, varies between locations and also between individuals assigned as Gulf of Mexico and Mediterranean origin based on otolith microchemistry (Figure 4.2, 4.3). These results will be compared with frequency of introgressed mitochondrial haplotypes.

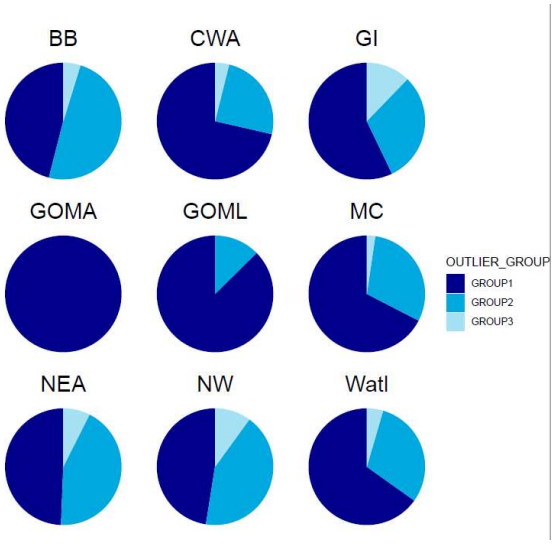

Figure 4.3. *Frequency of individuals belonging to each of the three differentiated groups based on genetic variability of adaptive markers at each location. Catch locations are indicated as GOMA= Adults from the Gulf of Mexico, GOML= Larvae from the Gulf of Mexico, WA= West Atlantic, CWA= Central West Atlantic, NEA= North East Atlantic, NW = Norwegian Sea, BB = Bay of Biscay, GI=Strait of Gibraltar, MC= Canary Islands. The different groups are represented in different colors as shown in the legend.*

4.3.4 Population structure of Atlantic bluefin tuna based on Copy number Variants (CNVs)

The obtained CNVs dataset from the Atlantic bluefin tuna RAD-seq data included 378 individuals and individual read counts for 1,604 CNVs. PCA based on this dataset differentiate two clusters: one comprised mainly by Mediterranean individuals, while the other showed sub-structuring of samples according to their corresponding group (groups are Mediterranean individuals, larvae from the Gulf of Mexico, adult spawners from the

Gulf of Mexico and larvae and young of the year from the Slope Sea) (Figure 4.4). However, this differentiation between groups corresponded to their inclusion at different libraries during the laboratory processing of the RAD-seq process (Figure 4.4). We therefore contacted the authors from the CNV discovery method (Dorant et al. 2020) to explore different hypothesis for the manner in which library effects could affect the final result. We are currently in contact with them searching for different solutions to this problem. Analysis of structural variants based on whole genome sequencing is awaiting the finishing of haplotype calling process.

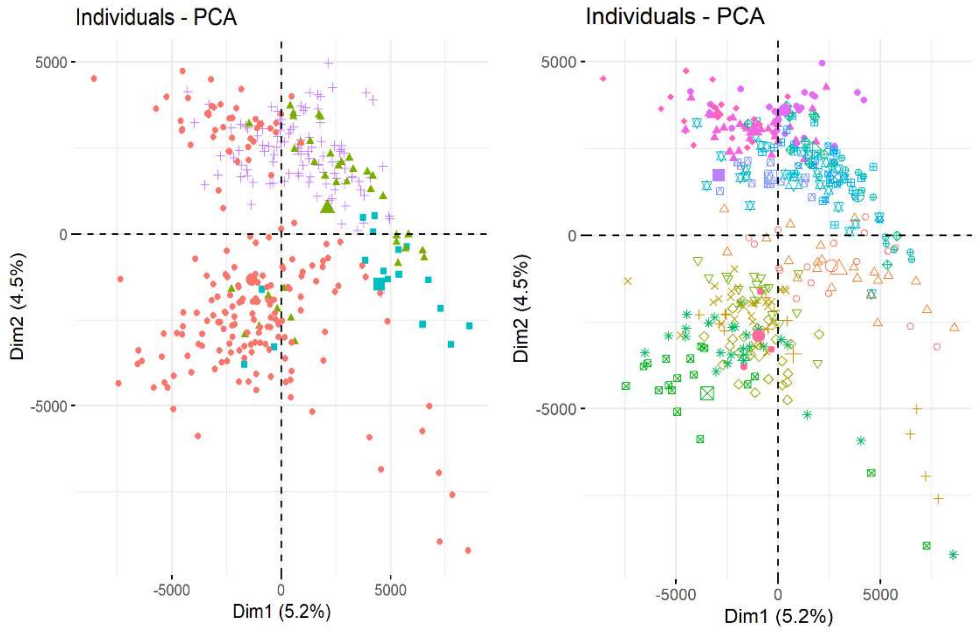

Figure 4.4. *PCA based on the 1,604 identified CNVs, where each point represents one individual. Individuals are colored by group (left: Mediterranean individuals, larvae from the Gulf of Mexico, spawning adults from the Gulf of Mexico and Slope Sea larvae and young of the year represented in red, blue, purple and green respectively) or by library pool (right).*

4.3.5 The inclusion of genetic markers adapted from Suda et al. 2019 represents a promising tool for genetic sex identification.

In total, 5 and 3 markers for genetic sex identification were included in the SNP array and the 96 SNP panel respectively. These markers had been adapted from sex-specific

markers designed in Suda et al. (2019) for Pacific bluefin tuna. Names and position in the reference genome of the Pacific bluefin tuna of designed markers for genetic sex identification are included in Table 4.3.

Table 4.3. *List of designed genetic markers adapted from (Suda et al. 2019). All the five markers are located within the scaffold_064 of the Pacific bluefin tuna genome, and position indicates the exact location of the target variant locus within this scaffold.*

	Position
SEX_IA	3,724,619
SEX_IB	3,724,625
SEX_IIA	3,726,480
SEX_IIB	3,726,477
SEX_III	3,724,698

From the SNP array results, the SEX_IIA genetic marker and 24 individuals were excluded due to high per SNP and per individual missing data rates respective (>0.3). Two most frequent genotype combinations were obtained based on the results of the 682 considered individuals, the first genotype combination is present in 367 individuals (Group 1) and the second combination is present in 213 individuals (Group 2). There were 8 other genotype combinations, two of them at only one or two alleles distance from the most frequent combinations (Table 4.4).

Among the genotyped samples, there are 151 and 101 individuals that had been visually identified respectively as males and females in the GBYP database, while the other 430 had unknown sex. The 87% of the individuals identified as females showed the Group 2 and Group 2 variant genotype combinations for sex markers, while the 76% of those identified as males showed the Group 1 combination (Figure 4.5).

Table 4.4. *Different genotype combinations obtained for the four genotype sex markers with the SNP array, and the number of individuals showing each of them (n). The two majoritarian combinations (Group 1 and Group 2) are shaded in grey. The rest of combinations are considered as variations (var) of one of these two majoritarian ones. Missing data is noted as "0/0".*

	SNP Array Sex Marker				
Genotype combination	SEX_I A	SEX_I B	SEX_II B	SEX_III	n
Group 1	GG	CC	TC	-/-	367
Group 1 - var 1	GG	CC	CC	-/-	4
Group 1 - var 2	GG	TC	TC	-/-	1
Group 2	TG	TT	CC	TAATGTA/-	213
Group 2 - var 1	TT	TT	CC	TAATGTA/-	38
Group 2 - var 2	TG	TT	CC	TAATGTA/TAATGTA	31
Group 2 - var 3	TT	TT	CC	TAATGTA/TAATGTA	18
Group 2 - var 4	TG	TC	CC	TAATGTA/-	7
Group 2 - var 5	TG	TT	TC	TAATGTA/-	2
Group 2 - var 6	TT	TC	CC	0/0	1

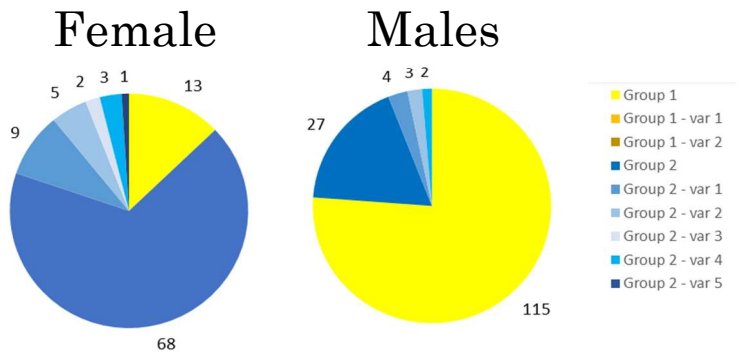

Figure 4.5. *Pie charts showing the proportions of individuals showing each genotype combination for sex markers included in the SNP array as shown in the legend that appear in the GBYP dataset as females, males and unknown.*

For the 96 SNP panel results, from the first test genotype plate of 94 samples, 91 individuals were kept for genetic sex identification analysis. Among them, 88 individuals

showed two most frequent genotype combinations (Combination 1 and Combination 2), while the other three showed two other combinations at only one allele distance from Combination 2 (Table 4.5).

Table 4.5. *Different genotype combinations obtained for the four genotype sex markers with the 96 SNP panel, and the number of individuals showing each of them (n). The two majoritarian combinations (Group 1 and Group 2) are shaded in grey. The rest of combinations are considered as variations (var) of one of these two majoritarian ones. Missing data is noted as "0/0".*

	96 SNP Panel Sex Marker – plate 1				
Genotype combination	SEX_IB	SEX_IIA	SEX_IIB	SEX_III	n
Combination 1	CT	AT	CC	TAATGTA/-	47
Combination 2	TT	TT	CC	TAATGTA/TAATGTA	41
Combination 2 – var 1	CT	TT	CC	TAATGTA/TAATGTA	2
Combination 2 – var 2	TT	TT	CC	TAATGTA/-	1
TOTAL					**91**

The marker SEX_IIB was no variable, and therefore no informative. Thus, it was excluded from the final 96 SNP panel configuration. Similarly, to what was observed from the SNP array data, the 97 % of the female individuals showed the genotype combination 2 (or variants of this combination), while the 80% of male individuals showed the genotype combination 1 (Figure 4.6).

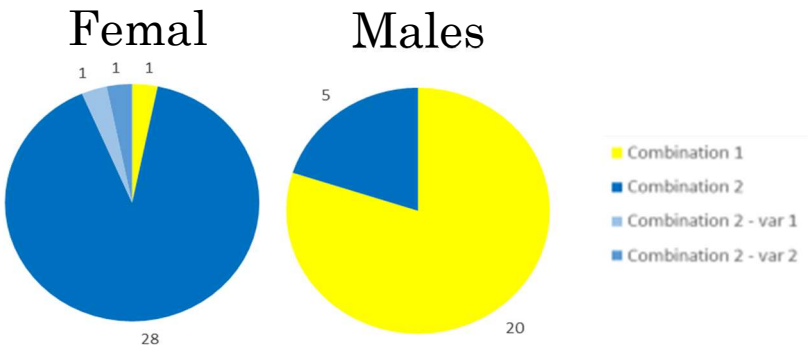

Figure 4.6. *Pie charts showing the proportions of individuals showing each genotype combination for sex markers included in the 96 SNP panel that appear in the GBYP dataset as females, males and unknown.*

Results obtained from genetic sex markers adapted from Suda et al. (2019) to the SNP array and the 96 SNP panel provided with similar results. In both cases the most frequent genotype combination in female individuals was more variable, which can be explained by the fact that the markers from which these were adapted were designed as male-specific (Suda et al. 2019) and may not recover all the possible variability among female individuals. Comparison of the most frequent genotype combination in visually identified female and male individuals obtained with both methods show some differences with the expected outcomes (Table 4.6). These differences can be explained by the fact that the absence (or scarcity) of homozygous individuals for the rarest allele (i.e., Individuals showing genotype TT for SEX_IA with the SNP array) could make the different genotypes difficult to assign.

Table 4.6. List of designed genetic markers adapted from (Suda et al. 2019). Expected genotypes for males (M) and females (F) according to the descriptions in Suda et al. (2019) and obtained genotypes considering the majoritarian genotype combinations for samples from each visually identified sex using markers adapted to the SNP array and the 96 SNP panel.

	Expected from Suda *et al.* 2019		SNP array		96 SNP panel	
	M	F	M	F	M	F
SEX_IA	GG	TT	GG	TG	-	-
SEX_IB	CC	TC/TT	CC	TT	CT	TT
SEX_IIA	AA	TT	-	-	AT	TT
SEX_IIB	TT	CC	TC	CC	CC	CC
SEX_III	-/-	TAATGTA/TAATGTA	-/-	TAATGTA /-	TAATGTA/-	TAATGTA / TAATGTA

These results show that sex markers adapted to the SNP array and the 96 SNP panel could be successfully used for genetic sex identification. However, there is a small percentage of individuals that would be genetically assigned to a different sex from that noted in the GBYP database. However, it should be further tested if these percentages of missasigned samples are due to a visual misidentification or to a failure of the genetic method.

4.3.6 Epigenetics

The results of this task are presented as a stand-alone document in Appendix I.

4.4 Conclusions

Population structure of Atlantic bluefin tuna:

- Our results confirm presence of two ancestry genetic profiles in Atlantic bluefin tuna
- Samples from the eastern side of the Atlantic (including feeding aggregates) are predominantly Mediterranean-like, whereas samples from the Western side are mostly Gulf of Mexico like (those from the Gulf of Mexico) or cover a wide range of profiles (Western and Central Atlantic)
- Additional conclusions on the population structure of Atlantic bluefin tuna will be derived from an integrated view when results from whole genome sequencing will be available.

Integration of genetic and otolith microchemistry data:

- Some samples are assigned to different origin based on otolith microchemistry and genetic markers, where the most common mismatch is Mediterranean genetic profile and Gulf of Mexico otolith origin. These individuals could correspond to individuals of Mediterranean origin performing early (yearling individuals) departures from the Mediterrranean Sea, or to individuals of different origin, such as alternative spawning areas used by eastern individuals, such as the Bay of Biscay.
- Analysis of individuals genetic profile suggests weaker and stronger stock mixing within the Eastern and Western stocks respectively than that concluded from otolith origin data.

Improvement of the 96 SNP traceability panel:

- The increased number of genotyped individuals provided with an enlarged reference dataset, which reflects better the genetic variability of the Atlantic Bluefin tuna and allowed to select better SNP markers for genetic origin traceability. The 96 SNP traceability panel was improved by including seven markers more informative for assignment than those that were removed.

Population mixing at foraging areas:

- Final conclusions on the population mixing behavior in foraging areas will be derived from an integrated view when genotyping results of 470 individuals with the final 96 SNP panel will be available.

Genetic markers for sex identification:

- Genetic markers for sex identification were successfully included in the origin traceability panel and genetic profile array, with a success rate of 80,55% with the SNP array and 89% with the 96 SNP panel (to be confirmed with additional samples).

Epigenetic approaches:

- The development of an epigenetic clock in Atlantic bluefin tuna requires a sampling scheme that ensure good representation of the species population in terms of environment, genetic component, sex and age classes
- The samples used in the development and testing of the method will be aged using otolith ring count analyses, which could bias the results if this ageing method is not considered accurate
- The method for CpG site identification should ensure that the best set of informative markers is found and for that aim the reduced representation or whole genome sequencing are the best approaches.
- The error rates from previous studies are high for the oldest specimens; using a large set of training samples, a good chronological ageing method and a large set of CpG sites will reduce this error.
- We should evaluate if the error rates expected (based on previous studies on long-lived species) are compatible with the application of the CKMR and if the reduced cost and logistics implied in epigenetic clock ageing compensate the implicit error rates.

References

Alexander, DH, J Novembre, K Lange. 2009. Fast model-based estimation of ancestry in unrelated individuals. Genome research 19:1655-1664.

Chiba, SN, S Ohashi, F Tanaka, A Suda, A Fujiwara, D Snodgrass, H Kiyofuji, K Satoh, N Suzuki. 2021. Effectiveness and potential application of sex-identification DNA markers in tunas. Marine Ecology Progress Series 659:175-184.

Dorant, Y, H Cayuela, K Wellband, M Laporte, Q Rougemont, C Mérot, E Normandeau, R Rochette, L Bernatchez. 2020. Copy number variants outperform SNPs to reveal genotype–temperature association in a marine species. Molecular Ecology 29:4765-4782.

Jombart, T. 2008. adegenet: a R package for the multivariate analysis of genetic markers. Bioinformatics 24:1403-1405.

Kavakiotis, I, A Triantafyllidis, D Ntelidou, P Alexandri, H-J Megens, RPMA Crooijmans, MAM Groenen, G Tsoumakas, I Vlahavas. 2015. TRES: Identification of Discriminatory and Informative SNPs from Population Genomic Data. Journal of Heredity 106:672-676.

Lischer, HEL, L Excoffier. 2011. PGDSpider: an automated data conversion tool for connecting population genetics and genomics programs. Bioinformatics 28:298-299.

Mayne, B, T Espinoza, D Roberts, GL Butler, S Brooks, D Korbie, S Jarman. 2021. Nonlethal age estimation of three threatened fish species using DNA methylation: Australian lungfish, Murray cod and Mary River cod. Molecular Ecology Resources n/a.

Purcell, S, B Neale, K Todd-Brown, et al. 2007. PLINK: A Tool Set for Whole-Genome Association and Population-Based Linkage Analyses. The American Journal of Human Genetics 81:559-575.

Rodríguez-Ezpeleta, N, N Díaz-Arce, JF Walter III, et al. 2019. Determining natal origin for improved management of Atlantic bluefin tuna. Frontiers in Ecology and the Environment 17:439-444.

Suda, A, I Nishiki, Y Iwasaki, A Matsuura, T Akita, N Suzuki, A Fujiwara. 2019. Improvement of the Pacific bluefin tuna (Thunnus orientalis) reference genome and development of male-specific DNA markers. Scientific Reports 9:14450.

Therkildsen, NO, SR Palumbi. 2017. Practical low-coverage genomewide sequencing of hundreds of individually barcoded samples for population and evolutionary genomics in nonmodel species. Molecular ecology resources 17:194-208.

Van der Auwera, GA, BD O'Connor. 2020. Genomics in the cloud: using Docker, GATK, and WDL in Terra: O'Reilly Media.

Yang, J, SH Lee, ME Goddard, PM Visscher. 2011. GCTA: A Tool for Genome-wide Complex Trait Analysis. The American Journal of Human Genetics 88:76-82.

5. DETERMINATION OF ANNUAL PERIODICITY IN ANNULI FORMATION IN ATLANTIC BLUEFIN TUNA OTOLITHS.

Task leader:
Enrique Rodriguez-Marin (CNIEO-CSIC)
Participants:

AZTI: Patricia L. Luque

CNIEO-CSIC: Isabel Castillo, Aida Parejo

SABS-FOC: Dheeraj S. Busawon, Alex Hanke, Nathan Stewart

5.1 Introduction

The description of the life cycle and effective management of Atlantic bluefin tuna (*Thunnus thynnus,* ABFT) requires comprehensive age and growth studies. One of the most widely used methods for estimating the age of ABFT has been based on the examination of calcified structures. The estimation of absolute age by reading otoliths has been validated by the bomb radiocarbon method (Neilson and Campana, 2008) and the periodicity of the formation of the annual increments by measuring otolith strontium: calcium ratio (Siskey et al., 2016).

Direct age assignment depends not only on the number of annuli found in the calcified structure, but also on the periodicity of annuli formation. In order to transform the band count into ages it is necessary to consider the marginal edge type related to the catch date and the birth date. The study by Siskey et al. (2016) that compares the periodicity of annulus formation in the otolith of ABFT against Sr:Ca oscillations, indicates that opaque bands occurs cyclically, consistent with seasonal cycles in Sr:Ca that serve as a proxy for seasonal temperatures variation (i.e. higher otolith Sr:Ca in opaque bands presuming to be formed during winter months) confirming the assumed inverse relationship between Sr uptake and temperature. In contrast, a higher strontium concentration was assayed in the translucent bands of otolith of southern bluefin tuna (*Thunnus maccoyii*) (Clear et al.,

2000) applying the same technique. Similarly, Sr concentrations were significantly higher in the translucent bands of the first dorsal fin spine (fin spine, hereafter) of ABFT (Luque et al., 2017), interpreting them as those formed in winter. In support to that, edge type and marginal increment analyses of the ABFT fin spines indicated a yearly periodicity of annulus formation with the translucent bands appearing in winter (Luque et al., 2014).

The periodicity of annuli formation is commonly determined by marginal increment analysis in which the distance from the growth annulus to the edge of the otolith is tracked over time. This method requires a good representation of observations throughout the year to detect any seasonality trend in the formation of growth bands (Campana, 2001; Panfili et al., 2002). The selected mark must be accurate enough to allow detection of its formation at the extreme edge of the otolith. Edge type identification, translucent or opaque, in otoliths of ABFT is difficult. The thickness of the section and the diffraction of light has been shown to influence the perception of the type of edge making the identification of marginal areas in the ABFT otoliths more difficult. Recently, it has been agreed that using transmitted light for otoliths direct ageing has improved marginal edge recognition (Rodriguez-Marin et al. 2020; 2021). However, long standing controversies remain regarding the periodicity, or seasonality, of otolith growth band formation which directly influences a correct age determination of ABFT using otoliths. Thereby, the aim of this work was to apply marginal increment analysis to determine the timing of band deposition. To address that, growth bands (annuli) were measured from otoliths of fish collected monthly. We also performed edge analysis by analyzing the change in the relative frequency of the opaque or translucent bands over the months.

5.2 Material and methods

To be able to effectively use the marginal increment analysis (MIA) method, sampling is required in all months of the year and, as far as possible, all ages in each month. The strong seasonality in the ABFT fisheries that mostly capture a limited size range, and the migratory behavior and the wide distribution area of this species, makes comprehensive

year-round sampling difficult. For this study, ABFT otoliths were collected from specimens obtained from both sides of the Atlantic Ocean and the Mediterranean Sea, thanks to extensive sampling by the Atlantic-Wide Research Programme for Bluefin Tuna of the International Commission for the Conservation of Atlantic Tunas (GBYP, ICCAT), the contributions of St. Andrews Biological Station (SABS) and the Spanish Institute of Oceanography National Center (CN-IEO). The sampling covered the years from 2009 to 2021 and a variety of fishing gears. Fish were measured mostly at straight fork length (SFL), but also at curved fork length, snout length and round weight. The latter measurements were transformed into SFL, following the biometric relationships established by ICCAT (Secor et al., 2015; Rodriguez-Marin et al., 2015). The size range sampled was from 50 to 295 cm SFL.

Otoliths were prepared by three laboratories (Fish Ageing Services (FAS), SABS and CN-IEO) following the standardized methodology described in Rodriguez-Marin et al. (2020). Three research centers read and analyzed the samples (SABS, CN-IEO and AZTI) also using the standardized reading criterion (Rodriguez-Marin et al., 2020). However, to better cover the sampling of months and size range, otoliths read with the reading criterion of Busawon et al. (2015) were also used. Both criteria differ mainly in that the opaque bands at the otolith edge are only counted if it was completely formed, following the first criterion, and are counted, even if not complete, following the second one. As such, to use the same band counting criteria to all samples, otolith readings using Busawon et al. (2015) criterion were adjusted as follow: if otolith edge was opaque, then number of bands = number of bands -1. The number of otoliths read applying the Busawon et al. (2015) criterion was 152, and for the Rodriguez-Marin et al. (2020) criterion was 2128.

The timing of band formation was assessed by examining the outermost edge of the ventral arm of the otolith section. Following the recommendation from Campana (2001), a minimum of two complete cycles needs to be examined, therefore, the periodicity in annulus deposition or MIA, was determined using the index of completion $C = W_n / ((W_{n-1}+W_{n-2})/2) \times 100$ (Tanabe et al., 2003); where Wn is the width of the marginal increment (distance from the end of the last opaque zone to the marginal edge, whatever edge nature); and Wn-1 and Wn-2 are widths of the previously completed increments (the distance from the end of the second or third most outer opaque zones to the last and

penultimate opaque zone). This method only allows the analysis of MIA in otoliths of specimens over two years old, for specimens older than one year, only one complete cycle was be used ($C = W_n / W_{n-1} \times 100$). Measurements were performed with a digital image analysis system. Otoliths were measured along an axis in the area between the sulcus margin and the ventral groove of the ventral arm where the annuli are most distinct, using a standardized "measurement line" (Rodriguez-Marin et al. 2020) (Figure 5.1).

Five readers participated in the measurements, although one of them read with both types of light, transmitted and reflected. This reader was considered as two different readers according to the type of light. This resulted in a total of 6 readers. The number of images read with transmitted light were 1740 and with reflected light to 540. Readers were requested to provide in their reading exercises the following information by sample: Light type (reflected, transmitted), number of annual bands (opaque), reading criterion (1 Busawon et al., 2015; 2 Rodriguez-Marin et al., 2020), ventral arm marginal edge type (wide translucent, narrow translucent or opaque), edge type confidence (1= no confident; 2= confident in completeness and not with the type and 3= confident), readability code (1= pattern present-no meaning, 2= pattern present-unsure with age estimate, 3= good pattern present-slightly unsure in some areas, 4= good pattern-confident with age estimate), Wn, Wn-1 and Wn-2 widths in mm, agreed band count (Yes for agreed and No for individual decision), agreed edge type (Yes for agreed and No for individual decision), measuring date, reader coding and notes with observations about the sample. The agreement fields were used because all samples have been previously read by expert readers as part of several ageing exercise exchanges or read by FAS, however we did not want to restrict new readers to the pre-assigned band counts if they didn't agree with the originally assigned band count or marginal edge type. An agreement with previous readings of 49% in the number of bands (were mostly +/- 1 band) and 50% in the type of edge (with the three categories) was reached.

A total of 2280 Atlantic bluefin tuna otolith images were analyzed to determine annual periodicity of annulus formation. Approximately 8% of the available samples had to be excluded from the study due to image quality, missing measurements, age (age 0), miss-match between number of bands and SFL. Furthermore, 18 samples were identified as outliers using the following criteria: if Wn > Wn-1 > Wn-2 and the index of completion C

was greater than 120%, were re-ordered Wn<Wn1<Wn2. The total number of samples available was 2101, with a good representation by age (number of bands) and by month, except for months 2,3 and 4 (Figure 5.2).

The index of completion was also analyzed using General Additive Models (GAMs) to evaluate the importance of variables such as month, age/size, reading criteria, light type and reader. The following transformations were applied to the data prior to fitting the GAMs: to account for cases where C was greater than 100, samples with an index of completion of 100 were changed 99.9. Edge type was not included in the model since it represents phases of completion and is essentially a derivative of the index of completion, that is the completion index for NT<WT<O. Formulations of the model with light effect as a random effect showed similar trends that differed slightly in the peak of completion, with rate of completion being the highest in July for reflected light vs. September for transmitted light. Since the trends were similar and the fact that the reflected light trend was not very informative due to the timing/span of sample collection, light type was excluded from the final model. Furthermore, the final model was fitted using both straight fork length and age, however SFL showed better fit compared to age. This better fit is likely due to length being a more continuous variable compared to age or number of bands. GAMs were fitted assuming beta distributed data for the response with a logit link A cyclic cubic spline basis function was specified for smoothers involving month of capture and was limited to 8 knots. Reader, Age and SFL were included as random effects. The best fitted GAM was:

Model: C~ s(Month,k=8) + s (SFL) + s(Reader).

5.3 Results and discussion

The Index of Completion by number of bands (considered presumably formed annually) shows an increase of C with the number of bands, although there is a clear change in the slope of this line, forming three groups: from 1 to 6 bands, from 7 to 16 band and more than 16 bands (Figure 5.3). These three slope sections made us explore MIA and edge type analyses with all annual/age bands grouped together and by the band groups or bins described above.

The trend in index of completion (C) appeared to be bimodal, indicating highest rate of completion in April and August to October (Figure 5.4). The bimodal trend is likely due to limited number of samples analyzed from January to April. When C is analyzed by age group, this bimodality continues to be observed, with June and July again showing the lowest values indicating that the otolith margin stops growing in these months. The maximum C values of the first months are supported by few samples, while the maximum values of the months from mid-summer to mid-fall are well sampled and indicate higher completion index values for the months of August-September through November. This is especially evident in the 7 to 16 age group, which is the best sampled group (Figure 5.5).

When the type of edge is analyzed, the month of greatest change in the ratio of translucent (narrow and wide) to opaque bands indicates the formation of opaque bands, this occurred between July and August in the overall marginal status (Figure 5.6) and from June to July in the marginal estate figure by age group 2 (7-16 years, Figure 5.7). This indicates that the opaque bands begin to form in July and continue to form up until October. The translucent band starts to form in November and peaks in May and June with the highest percentage of wide translucent bands (Figure 5.6 and Figure 5.7).

In the completion index analysis and edge type analysis, there is consistency in the results between readers, between quality values in the identification of edge type (those with the highest and lowest confidence in quality) and according to the type of light (reflected or transmitted). Although in the type of light there is a difference in the month of August, where with transmitted light the opaque marginal edge represented nearly 20%, while with reflected light it represented 70%.

The functional relationship between month of capture and index of completion obtained from the GAM model, shows that the maximum C was obtained in the month of September and from this month onwards it decreases until reaching a minimum value in May (Figure 5.8). The trend represents the population-level predicted values and their corresponding confidence intervals (i.e., the uncertainty related to the variance parameters for the mean

random effects associated with Reader and SFL are not included). The variability associated with the month of capture is relatively small compared to sources such as reader (Table 5.1). Nevertheless, there is evidence for the level of completion to be highest in September. The factors Month, Age, SFL and Reader accounted for a significant amount of the variability in the index of completion. Diagnostics plots for the GAM model indicated no issues (Figure 5.9 and Figure 5.10). The model explained 47.3% of the variation in the dataset with a R^2 of 0.464.

Each annulus consists of a translucent and opaque band. Since our completion index is based on the measurement between the end of consecutive opaque bands, the minimum value of C from MIA and GAM model after the maximum values of August and October would indicate that the opaque band would finish forming in November. This is also supported by the analysis of the edge type which indicates that the opaque band finishes forming in the same month. From the end of the year and the beginning of the following year there is minimal marginal edge growth and this is when the translucent band begins to form and reaches its maximum development in June.

If we go with the hypothesis that the MIA suggests, it is that the highest proportion of increments are completed (based on counts of complete opaque zones) by November 30, then this should be our adjustment date because in the ageing protocol opaque zones are only counted once they are complete. The adjustment is made with the marginal edge type identified in the otolith and accordingly must be applied to obtain the adjusted age. This would mean to delay the current date of the July 1st adjustment criterion (Rodriguez-Marin et al., 2020) to November 31. This formation of the otolith edge type would be in agreement with the patterns found in ABFT fin spines (Luque et al., 2014).

To see the influence of applying the current age adjustment criterion (Rodriguez-Marin et al., 2020) and the new one proposed in this study, we used the current ICCAT length at age database to see how the cohorts were reflected using the otolith readings available in that database, and in particular to see how it influenced the location of the strong 2003 year class (Rodriguez-Marin et al 2022). The change in the date of the otolith fitting criterion allows for a better outline of the strong 2003 year class (Figure 5.11).

The new adjustment criterion applied to the ICCAT length at age database also allows us to obtain a new growth curve. The growth curves obtained from both calcified structures (fin spines and otoliths) and from otoliths only, show little difference, at most one year, with the growth functions currently applied to the eastern (Cort 1991) and western (Ailloud et al., 2017) ABFT stocks (Figure 5.12). In this figure are represented all the ages that appear in the ALKs and are included in the age range from 0 to 22 years.

5.4 Conclusions

Completion index and marginal edge analyses has evidenced that the annulus, including a translucent band followed by an opaque band, is formed in November in the Atlantic Bluefin tuna otolith. Hence, we consider that this month is our adjustment date because in the ageing protocol opaque zones are only counted once they are complete. This would mean to delay the date of the current July 1st adjustment criterion to November 30.

Table 5.1. The variance and standard deviation for each smooth in the final GAM model.

Component	Variance	Std_dev	Lower_ci	Upper_ci
Month	0.0108	0.104	0.0378	0.287
SFL	0.00000936	0.00306	0.00143	0.00654
Reader	0.266	0.516	0.250	1.06

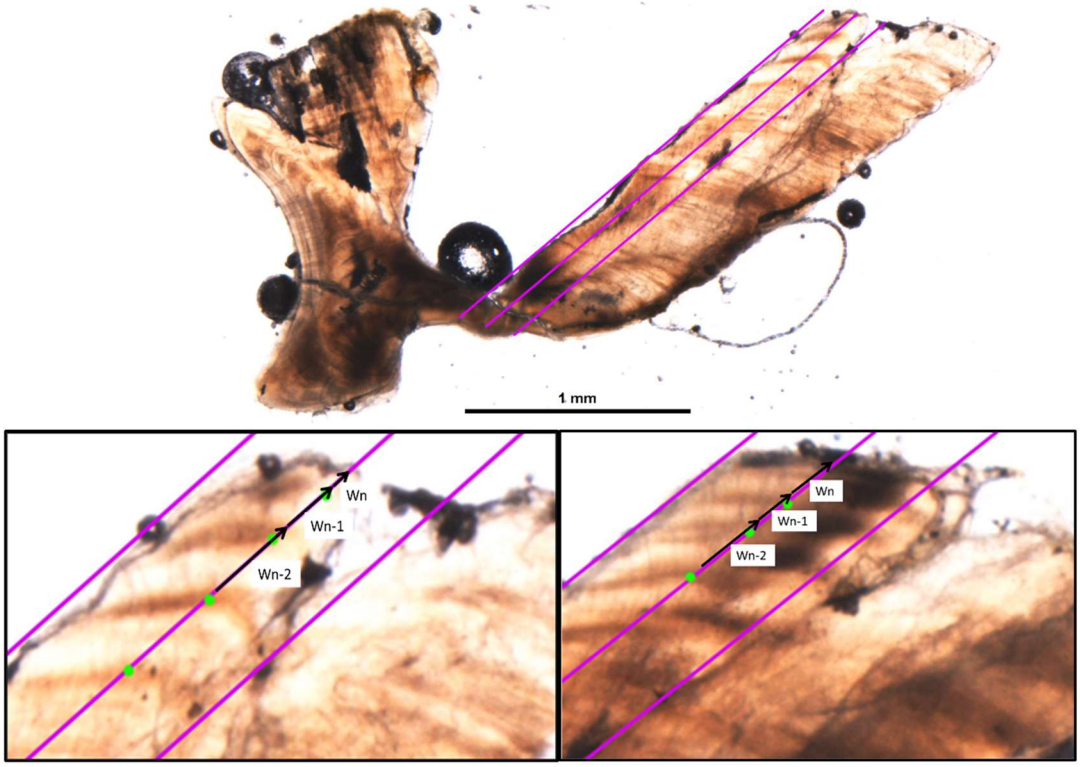

Figure 5.1. Bluefin tuna otolith showing measurement lines (top) and Wn-2, Wn-1 and Wn measurements identified with black arrows (bottom). The green dots indicate the opaque bands identified as having annual deposition. Bottom left is a 6 year old individual with a narrow translucent edge and on the bottom right is a 5 year old individual with an opaque marginal edge.

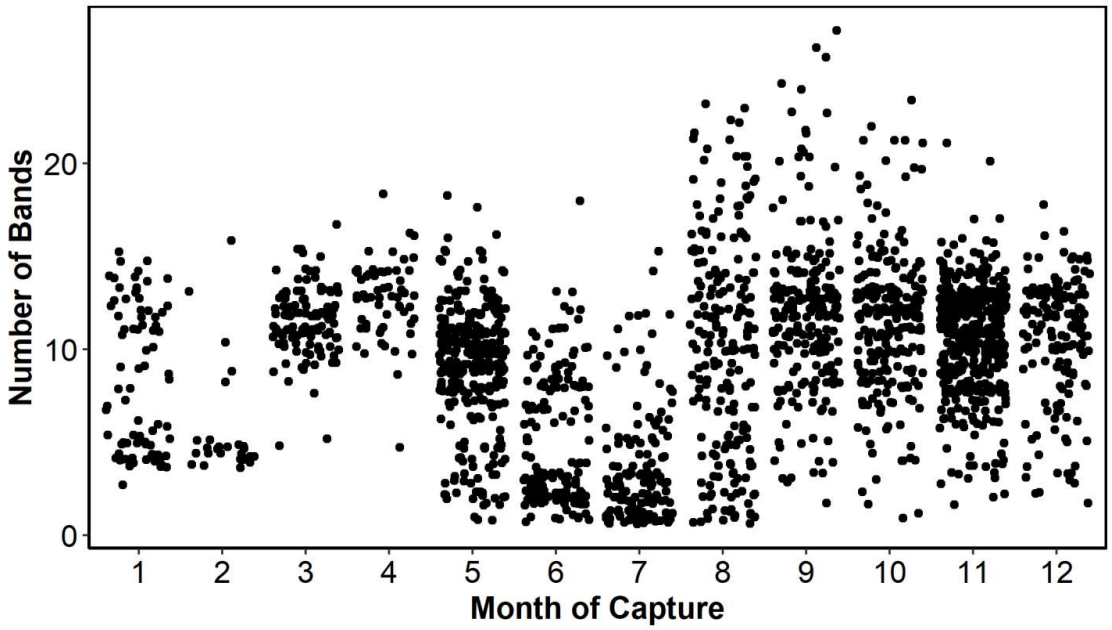

Figure 5.2. Number of samples identified by number of bands and month of capture.

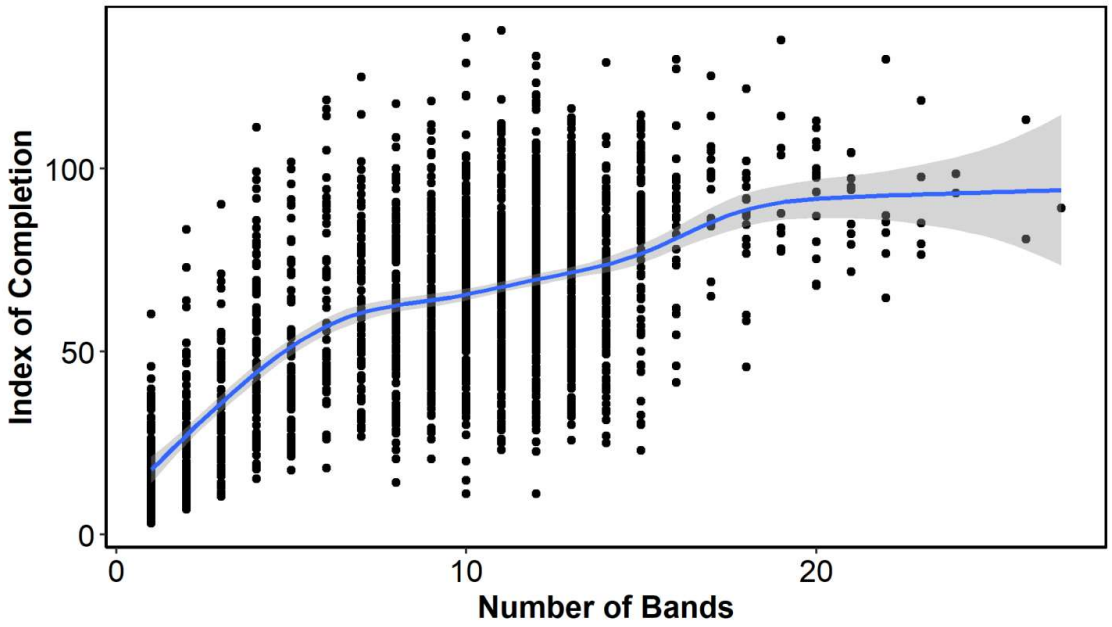

Figure 5.3. Index of Completion by number of annual bands.

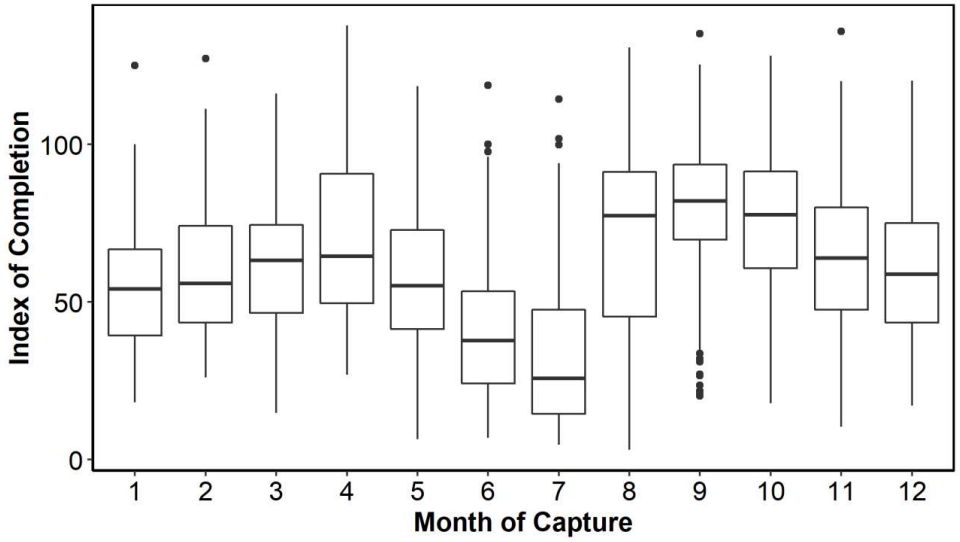

Figure 5.4. Mean index of completion (C) by month.

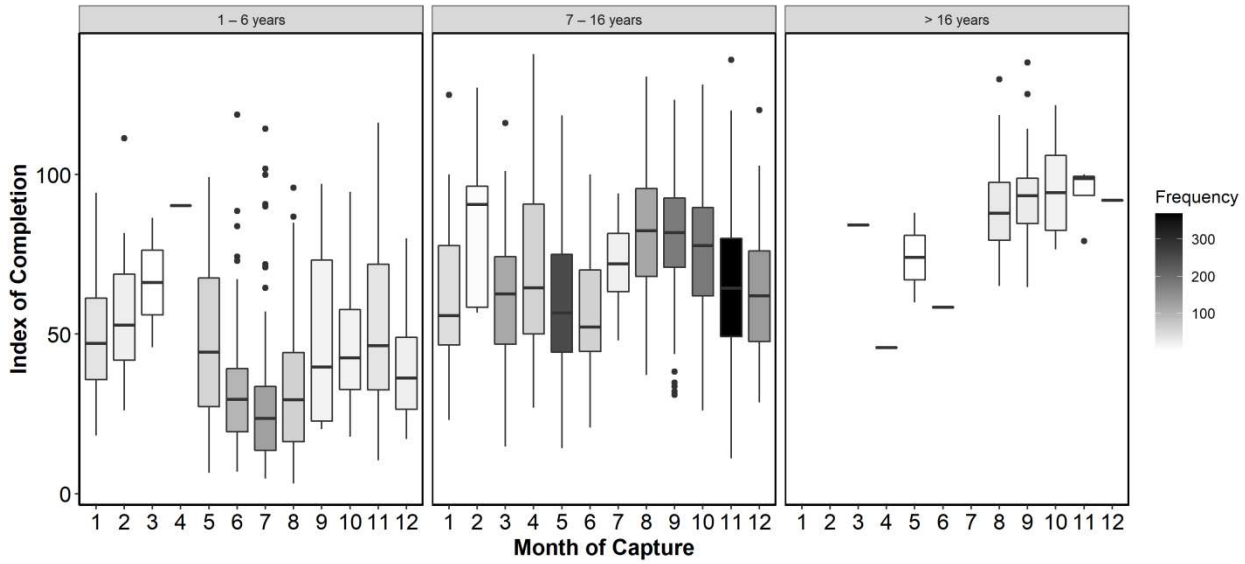

Figure 5.5. Mean index of completion (C) by month and age group (number of annual bands binned). The gray scale indicates the number of samples analyzed. Months 3- 4 for bin 1, month 2 for bin 2 and months 11-7 for bin 3 have a low number of samples (5 or less).

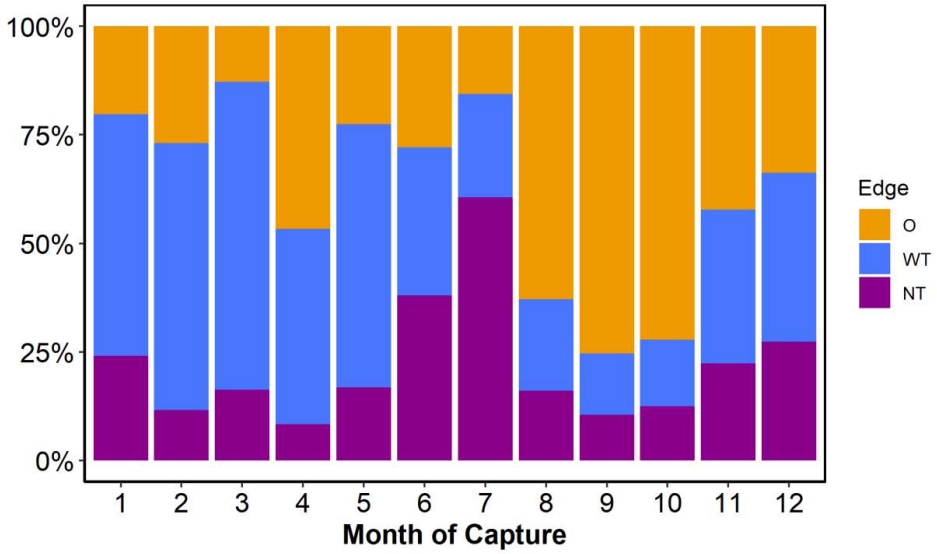

Figure 5.6. Percent edge type by month.

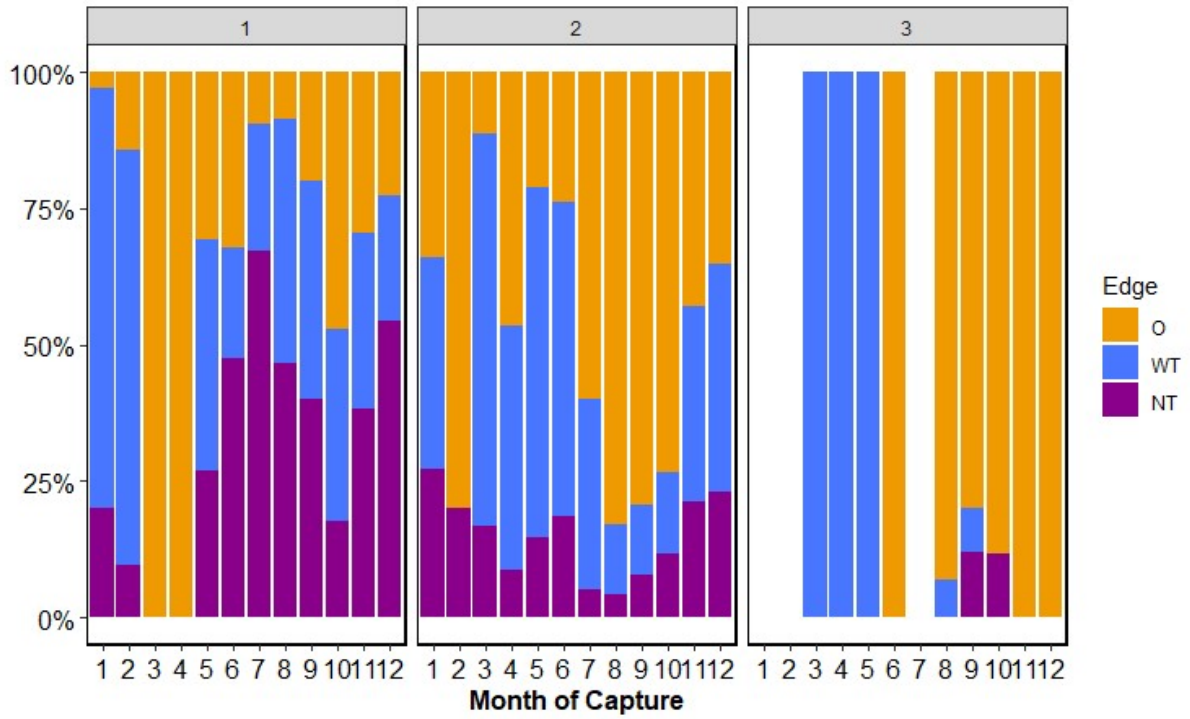

Figure 5.7. Marginal state by month and number of bands bin (age). Months 3- 4 for bin 1, month 2 for bin 2 and months 11-7 for bin 3 have a low number of samples (5 or less).

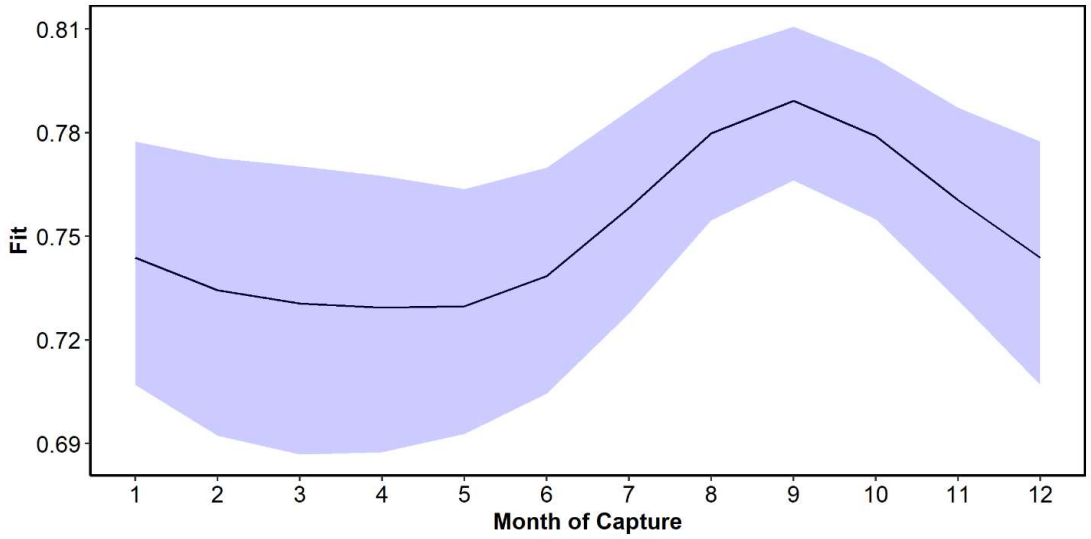

Figure 5.8. Prediction interval for the Month of Capture effect from the GAM model .

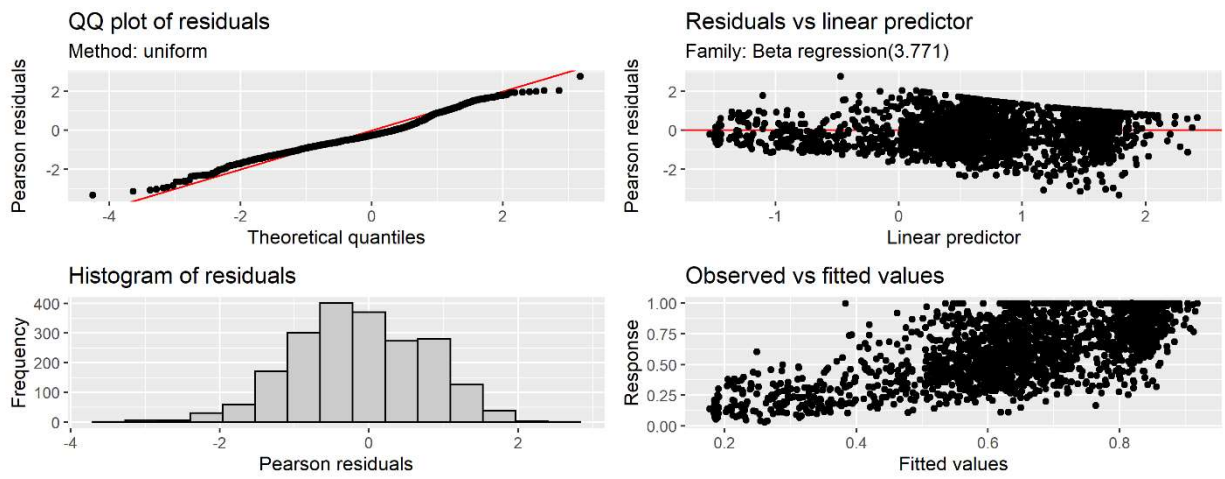

Figure 5.9. Diagnostic plots for the final GAM model. The QQ-plot and the histogram of the residuals are used to verify normality. The plot of standardized residuals against fitted values assesses homogeneity.

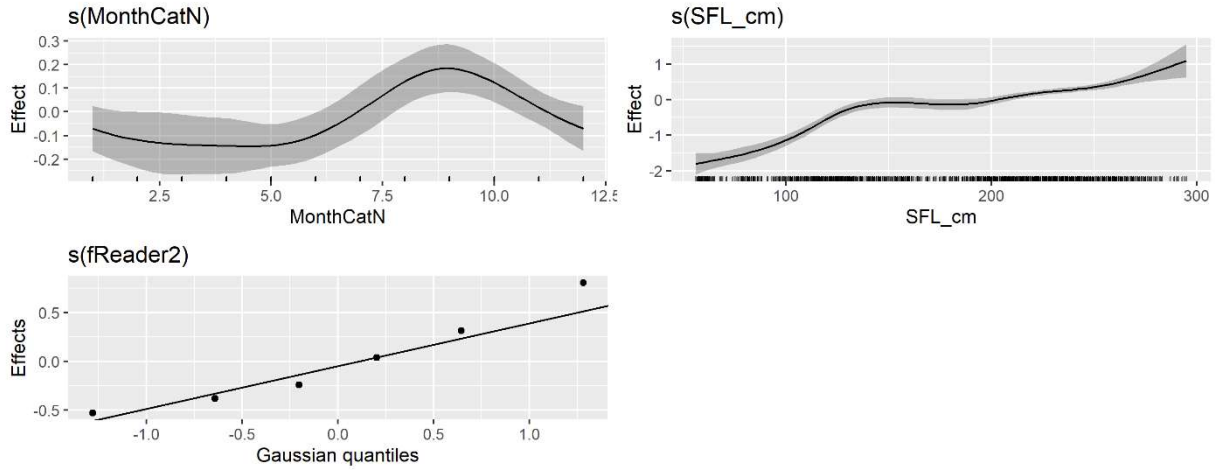

Figure 5.10. Estimated smoothing effects obtained by the GAM model.

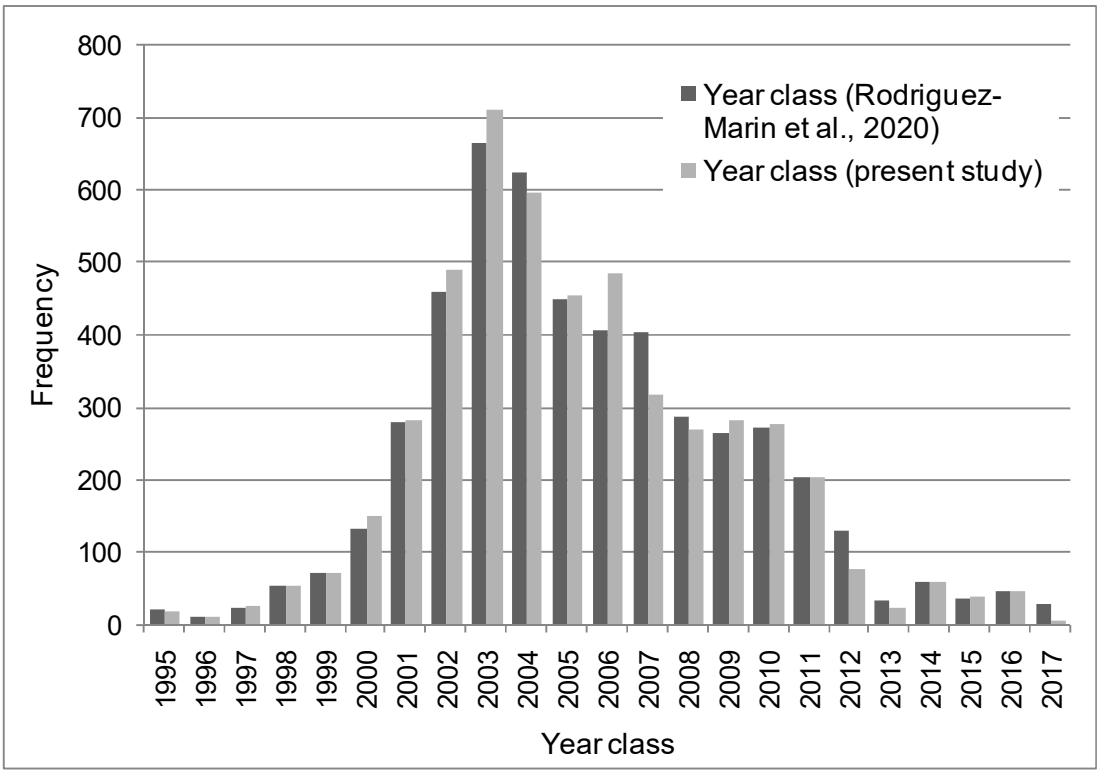

Figure 5.11. Number of Atlantic bluefin tuna by year class by applying the current (Rodriguez-Marin et al., 2020) and new age adjustment criteria to otolith band counts.

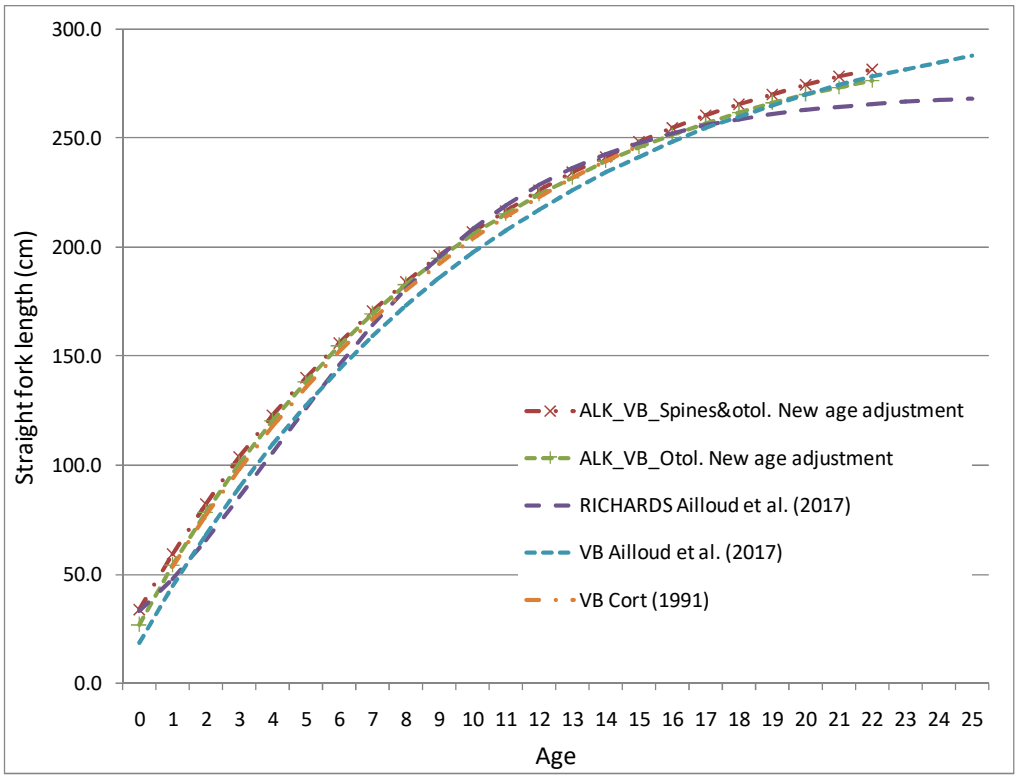

Figure 5.12 Growth curves obtained from the age-length keys (ALK) of the ICCAT database by applying the new age adjustment criterion (conversion of number of bands into ages). Both ALks growth functions (one using all the available calcified structures: fin spines and otoliths, and another using only the otoliths) are represented together with the growth curves currently applied to both stocks of Atlantic bluefin tuna. VB represents the von Bertalanffy fit to the length at age data.

References

Ailloud, Lisa E., Matthew V. Lauretta, Alex R. Hanke, Walter J. Golet, Robert J. Allman, Matthew R. Siskey, David H. Secor, and John M. Hoenig. 2017. Improving growth estimates for Western Atlantic bluefin tuna using an integrated modeling approach. Fish Res, 191: 17-24.

Busawon, D.S., Rodriguez-Marin, E., Luque, P.L., Allman, R., Gahagan, B., Golet, W., Koob, E., Siskey, M., Ruiz, M., Quelle, P., Neilson, J.D., Secor, D.H. Evaluation of an Atlantic bluefin tuna otolith reference collection. Collect. Vol. Sci. Pap. ICCAT. 2015, 71, 960-982

Campana SE. Accuracy, precision and quality control in age determination including a review of the use and abuse of age validation methods. J Fish Biol. 2001, 59:197-242.

Clear NP, Gunn JS, Rees AJ. Direct validation of annual increments in the otoliths of juvenile southern bluefin tuna, *Thunnus maccoyii*, by means of a large-scale mark-recapture experiment with strontium chloride. Fish Bull. 2000, 98:25-40.

Cort, J. L. (1991). Age and growth of bluefin tuna Thunnus thynnus (L.) of the Northeast Atlantic. ICCAT Collective Volume of Scientific Papers 35, 213–230.

Luque P, Rodriguez-Marin E, Landa J, Ruiz M, Quelle P, Macias D, et al. Direct ageing of Thunnus thynnus from the eastern Atlantic Ocean and western Mediterranean Sea using dorsal fin spines. J Fish Biol. 2014, 84:1876-903.

Luque PL, Zhang S, Rooker JR, Bidegain G, Rodriguez-Marin E. Dorsal fin spines as a non-invasive alternative calcified structure for microelemental studies in Atlantic bluefin tuna. Journal of Experimental Marine Biology and Ecology. 2017, 486:127-33. doi:http://dx.doi.org/10.1016/j.jembe.2016.09.016

Neilson JD, Campana SE. A validated description of age and growth of western Atlantic bluefin tuna (*Thunnus thynnus*). Canadian Journal of Fisheries and Aquatic Science. 2008, 65:1523-7

Panfili, J., de Pontual, H., Troadec, H., Wright, P.J. Manual of Fish Sclerochronology, co-edition. IFREMER-IRD, Brest, 2002, pp. 464.

Rodriguez-Marin, E., Busawon, D., Addis, P., Allman, R., Bellodi, A., Castillo, I., Garibaldi, F., Karakulak, S., Luque, P.L., Parejo, A., Quelle, P. Calibration of Atlantic bluefin tuna otolith reading conducted by an independent fish ageing laboratory

contracted by the ICCAT Research Programme GBYP. Collect. Vol. Sci. Pap. ICCAT, 2021, 78(3): 938-952.

Rodriguez-Marin E, Quelle P, Addis P, Alemany F, Bellodi A, Busawon D, et al. Report of the ICCAT GBYP international workshop on Atlantic bluefin tuna growth. Collect Vol Sci Pap ICCAT. 2020, 76:616-49.

Rodriguez-Marin E., Quelle P., Busawon D. Description of the ICCAT length at age data base for bluefin tuna from the eastern Atlantic, including the Mediterranean sea. 2022. ICCAT SCRS/2022/075

Rodriguez-Marin, E., Ortiz, M., Ortiz de Urbina, J.M., Quelle, P., Walter, J., Abid, N., Addis, P., Alot, E., Andrushchenko, I., Deguara, S., Di Natale, A., Gatt, M., Golet, W., Karakulak, S., Kimoto, A., Macias, D., Saber, S., Santos, M.N. dos, and Zarrad, R.. Atlantic bluefin tuna (Thunnus thynnus) Biometrics and Condition. PloS one. 2015, vol. 10, no 10, p. e0141478.

Secor, D. H., Busawon, D., Gahagan, B., Golet, W., Koob, E., Neilson, J., & Siskey, M. Conversion factors for Atlantic bluefin tuna fork length from measures of snout length and otolith mass. Collect. Vol. Sci. Pap. ICCAT. 2014, 70(2), 364-367.

Siskey M, Lyubchich V, Liang D, Piccoli P, Secor D. Periodicity of strontium: Calcium across annuli further validates otolith-ageing for Atlantic bluefin tuna (*Thunnus thynnus*). Fisheries Research. 2016, 177:13-7.

Tanabe, T., Kayama, S., Ogura, M., & Tanaka, S. Daily increment formation in otoliths of juvenile skipjack tuna *Katsuwonus pelamis*. Fisheries Science. 2003, 69(4), 731-7

6. OTOLITH CHEMISTRY

Task Leader:

Igaratza Fraile (AZTI), Jay Rooker (TAMUG) and Deirdre Brophy (GMIT)

Participants:

AZTI: Naiara Serrano, Iraide Artetxe

CNRS: Christophe Pecheyran, Fanny Claverie, Gaelle Barbotin

UNIVERSITY OF ARIZONA: David D. Dettman

EHU/UPV: Guillermo Garcia, Alfonso Estevas

GMIT: Elizabeth Tray, Louise Vaughan

NOAA: Beverly Barnett, Robert Allman, John Walter, Ashley Pacicco

6.1 Task 1: Improve the baseline for Mediterranean vs. Gulf of Mexico origin tuna combining stable isotope and trace element analyses

6.1.1 Introduction

Movement of Atlantic bluefin tuna across the 45°W management boundary has large implications for the stock assessment and management of the species. Otolith microchemical analyses have shown the potential to resolve questions regarding migrations patterns and stock mixing. In an attempt to further explore this technique, during the previous GBYP Phase 10, two-dimensional trace element maps were performed in otoliths of spawning adults captured in both sides of the Atlantic, Gulf of Mexico (GOM) and Mediterranean Sea (MED). Preliminary results suggested that within-otolith distribution pattern of Sr, Ba and Mg were distinct between the two stocks. Here, additional otoliths were analyzed, and machine learning techniques were applied to better discriminate between the eastern (MED) and western (GOM) components using otolith trace element distribution. Besides, the area of otolith transverse sections best discriminating between the two stocks was identified.

6.1.2 Material and Methods

Sagittal otoliths of 48 adult spawners from the Gulf of Mexico and Mediterranean Sea captured in spawning aggregations were selected as reference samples (Table 6.1.1). Additionally, 10 otoliths of bluefin tuna of unknown origin captured in Gulf of Saint Lawrence (N=1), Moroccan coast (N=4) and central North Atlantic (N=5) were selected to predict their nursery origin. Otoliths were cleaned with deionized water and dried under laminar air flow. One sagittal otolith from each bluefin tuna specimen was embedded in two-part epoxy resin and polished with silicon carbide sandpapers of a range of grit sizes under running water until the core was exposed.

Table 6.1.1.: Otoliths of adult bluefin tuna captured in spawning aggregations from the Gulf of Mexico and Mediterranean Sea selected for two-dimensional trace element analyses.

Area	Sub-area	Size-range (cm)	N
Gulf of Mexico		199-280	19
	Western	208-237	10
Mediterranean Sea	Central	209-239	10
	Eastern	141-287	9

Otoliths from the Gulf of Mexico and Mediterranean Sea were analyzed with laser ablation inductively coupled mass spectrometry (LA-ICPMS) (available at the Institut des Sciences Analytiques et de Physico-Chimie pour l'Environnement et les Matériaux, Université de Pau et des Pays de l'Adour/CNRS, Pau, France) by rastering across the sectioned otolith to create two dimensional maps of trace element concentration across the otolith sections. To correct for short-term instrumental drift, two standards (NIST-610 and NIST-612) were measured at the beginning and the end of each session. Measurement accuracy was determined based on an otolith certified reference material for trace elements (FEBS-1). Sr, Ba, Mg and Mn concentrations were measured on otolith transverse sections of 48 bluefin tuna from GOM (N=19) and MED (N=29). The laser beam was set to scan in a raster pattern mode over the surface of the ventral arm of the otolith. Two-dimensional images were built from the fs-LA-HR-ICPMS signal resulting from the

samples ablation according to a series of horizontal lines (e.g. Figs. 6.1.1 to 6.1.4). The data were saved as matrices, and calcium map was used in a pre-processing step to filter the signal of the aragonite. Concentrations of Sr, Ba, Mn and Mg were converted to color images to visualize trace element patterns. Of the 48 otoliths analyzed, one otolith from the central Mediterranean Sea was discarded from further analysis because part of the data was not recorded by the spectrometer. In a pre-processing step, all the images were moved, rotated to a specific coordinate and flipped if necessary to fit within a standard template. Then, the data corresponding to approximately the first year of life was selected using a second template, ensuring to exclude the border of the otolith sections, which contains material accreted during the adult stages (Fig. 6.1.5) (Fraile et al. 2015, Shiao et al. 2009). This pre-treatment of the data allowed to compare the same life period in all individuals studied, despite the different sizes and shapes of the otoliths. A neural network (NN) algorithm was developed with Matlab to train and test the proposed NN model, and to classify the individuals by combining the elemental concentrations in the otolith selected portion. Concentrations were split in categories (represented as colors), and binarized to be included as explanatory variables in a neural network discriminatory analysis. Using Matlab, a color threshold was used to binarize the images (Fig 6.1.6). The values of the input matrix were defined by the total number of pixels at different categories within the defined area. The NN was constructed using K fold cross validation (K=10). Data was split into training and testing data sets, and this process was repeated 10 times with each of the possible subsets of test data.

6.1.3 Results and Discussion

Visualization of elemental concentration distribution patterns in otoliths by means of two-dimensional imaging can provide key information to infer important life history events such migrations (e.g., movements across water masses with distinct physicochemical properties) and/or highlight ecological events. Besides, two-dimensional visualization of otolith section may be a useful approach to select the portion of the otoliths to be analyzed using LA-ICPMS, SIMS or other analytical techniques.

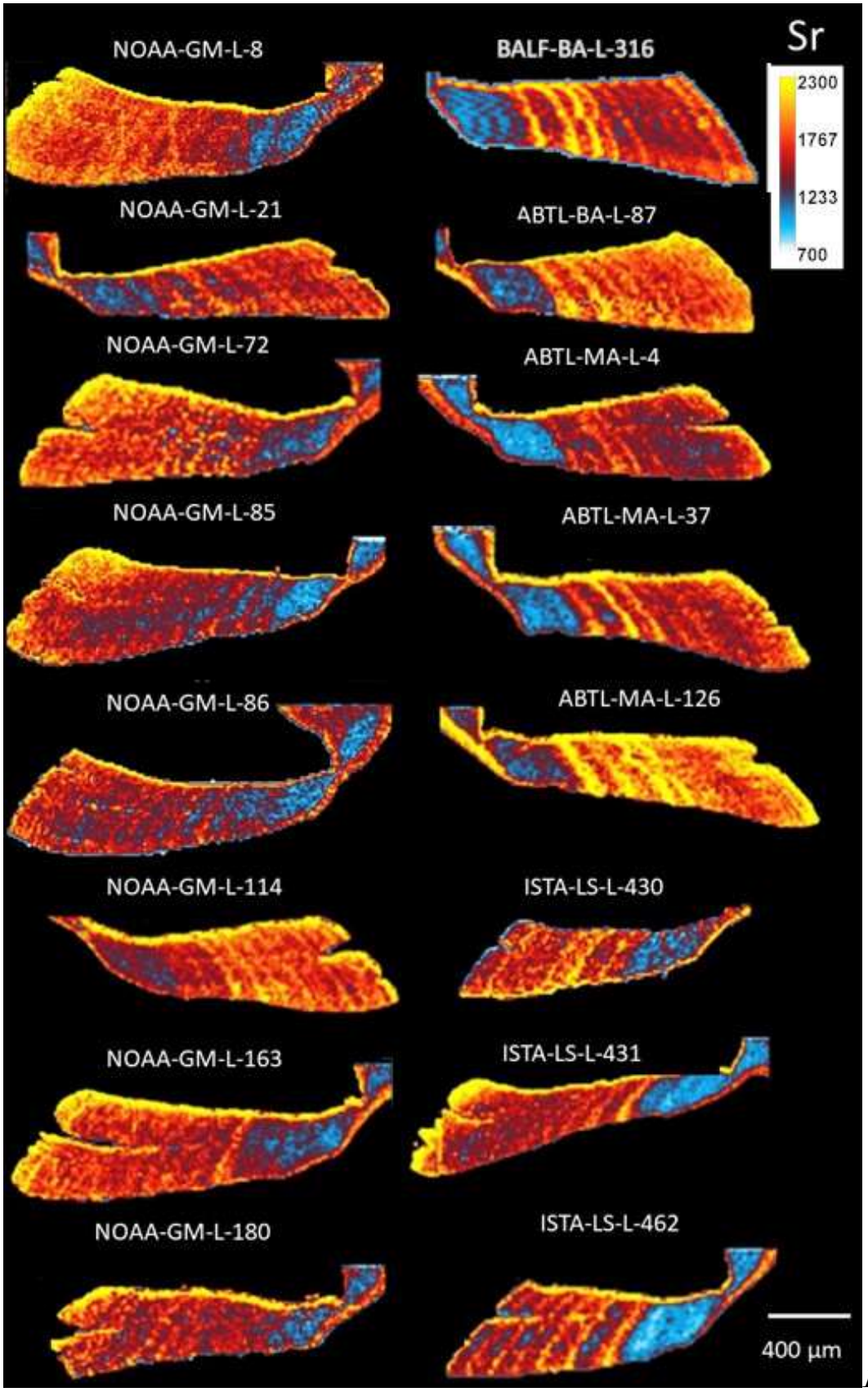

Figure 6.1.1: Two-dimensional maps of Sr concentration (in ppm) across otolith transverse sections of bluefin tuna from the Gulf of Mexico (left panel) and Mediterranean Sea (right panel).

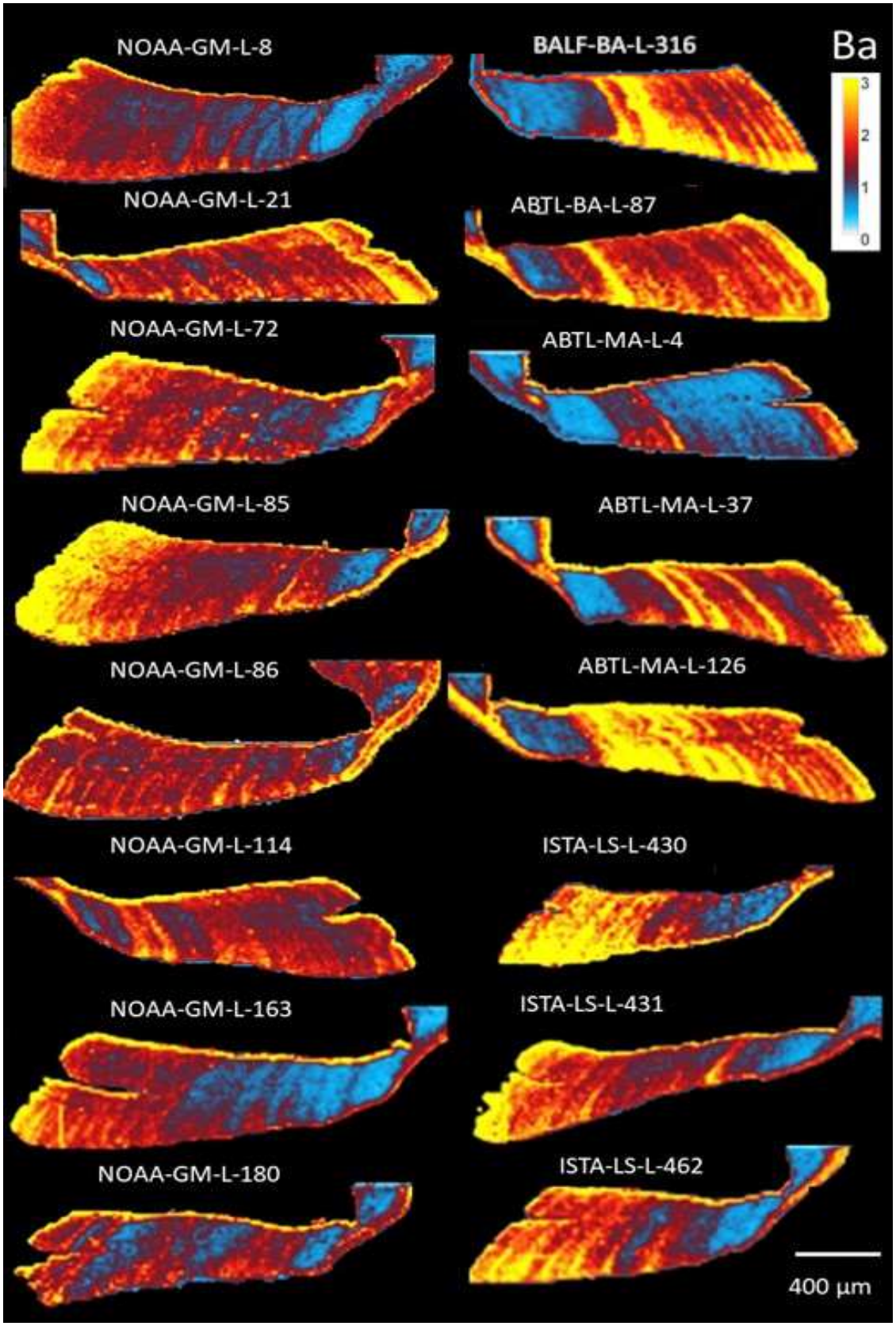

Figure 6.1.2: Two-dimensional maps of Ba concentration (in ppm) across otolith transverse sections of bluefin tuna from the Gulf of Mexico (left panel) and Mediterranean Sea (right panel).

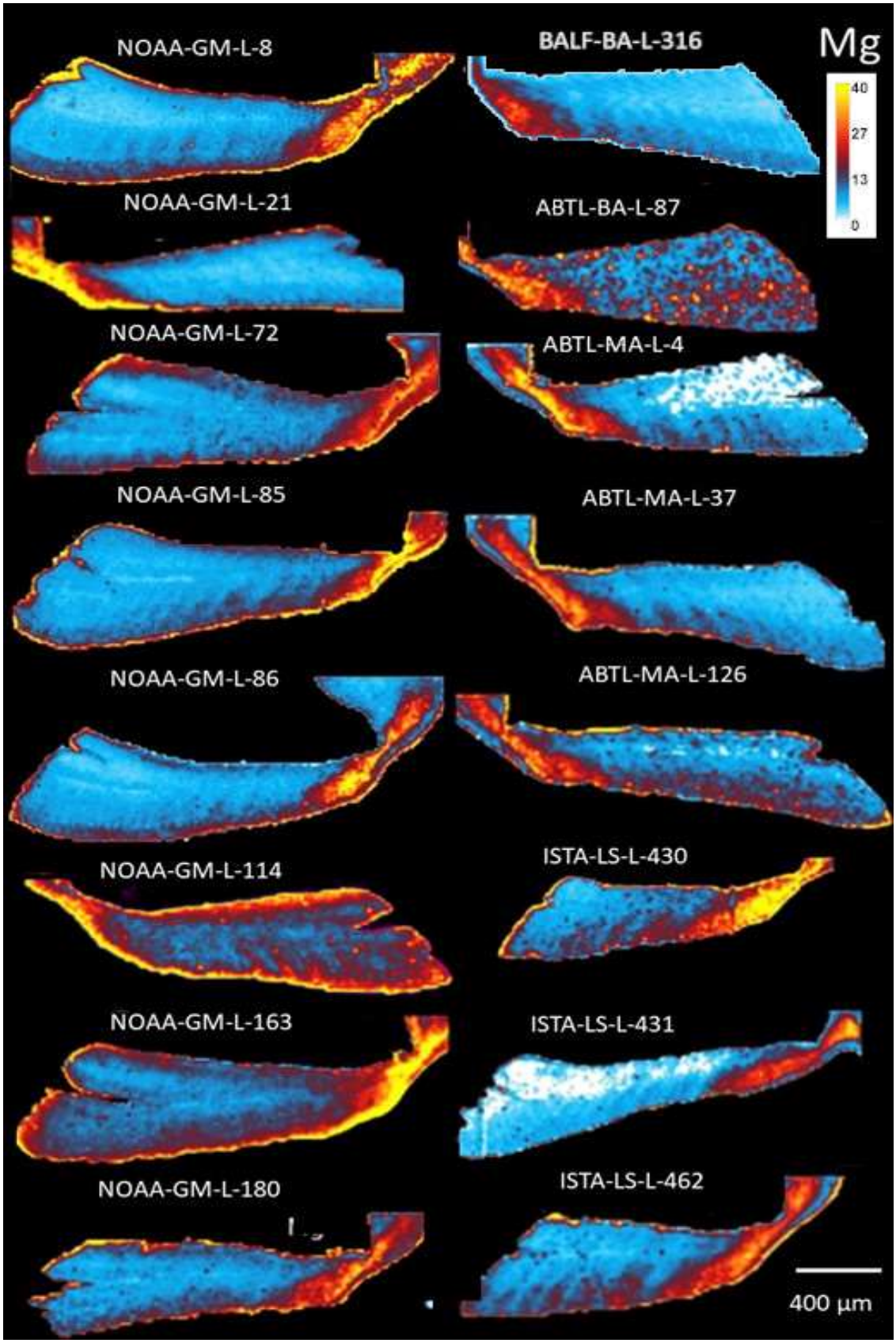

Figure 6.1.3: Two-dimensional maps of Mg concentration (in ppm) across otolith transverse sections of bluefin tuna from the Gulf of Mexico (left panel) and Mediterranean Sea (right panel).

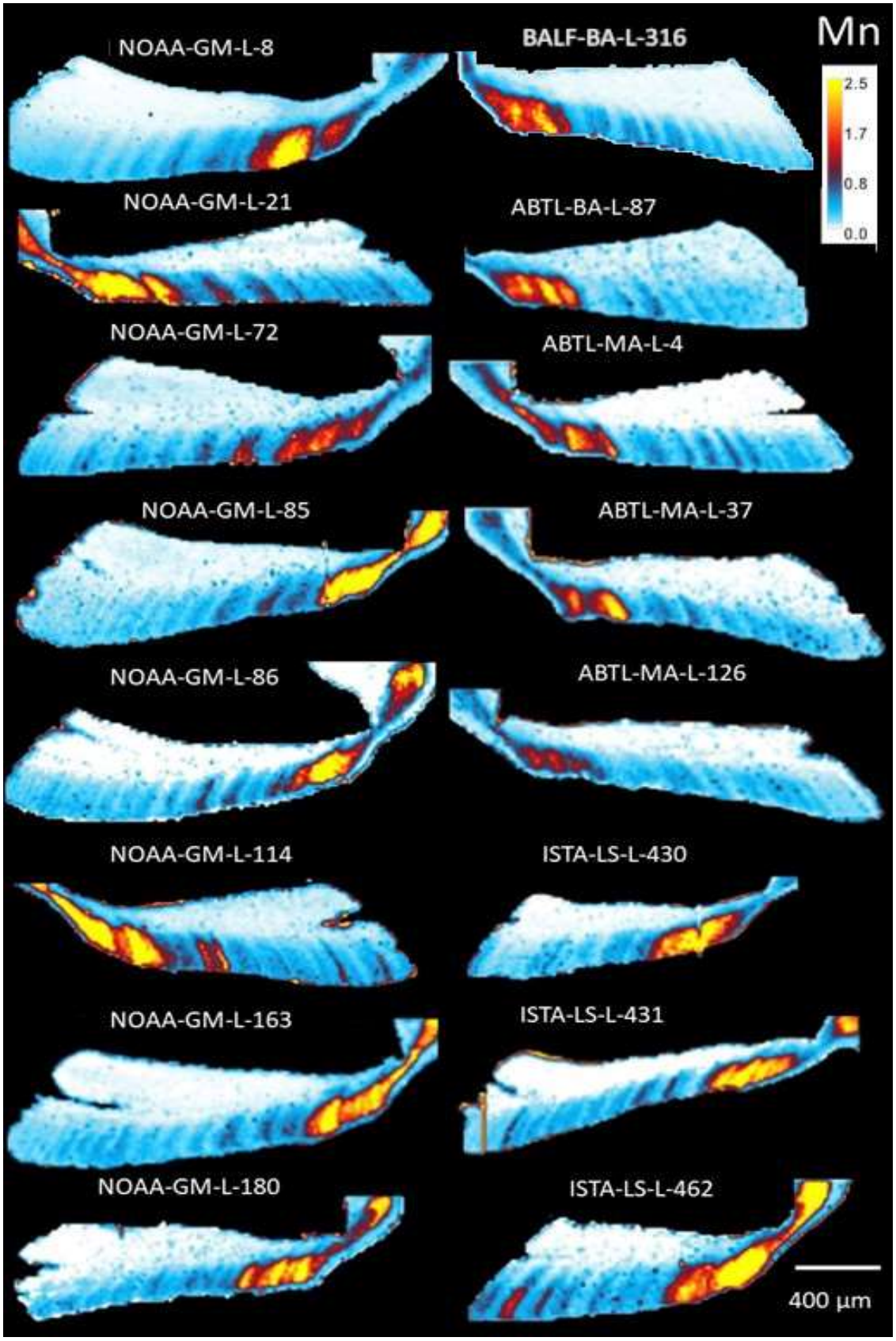

Figure 6.1.4: Two-dimensional maps of Mn concentration (in ppm) across otolith transverse sections of bluefin tuna from the Gulf of Mexico (left panel) and Mediterranean Sea (right panel).

During the current GBYP Phase, two-dimensional maps Ba, Mg, Mn and Sr were produced for 48 otoliths of bluefin tuna from the Gulf of Mexico (GOM) and Mediterranean (MED) nurseries (e.g. Figs. 6.1.1 to 6.1.4). In all otoliths analyzed, Sr and Ba concentrations were lower during the early life stages in both Mediterranean (MED) and Gulf of Mexico (GOM) bluefin tuna. A cyclicity in Sr and Ba concentrations was visible in most of the otoliths, presumably related to seasonal migrations between water masses. In contrast, Mg and Mn concentrations were highest at early life stages, and an abrupt decrease was observed after the first year. The results are concordant with previous findings showing that incorporation of Mn into fish otoliths is sensitive to growth (Limburg et al. 2011), and Mg concentration reflects metabolic activity of fish (Limburg et al. 2018). A cyclicity in Mn concentration was observed in some individuals, although Mn banding was attenuated with time. Differences in Mn patterns among individuals could be explained by different ecological strategies adopted by individual tuna.

Within this task, we propose an effective NN application to classify otolith elemental concentrations into two classes: bluefin tuna individuals from the eastern (MED) and western (GOM) nurseries. The model is first trained and then evaluated by employing tuna otoliths from Gulf of Mexico and Mediterranean Sea spawning aggregations. The neural network successfully predicted the origin of bluefin tuna with a classification accuracy of 98%.

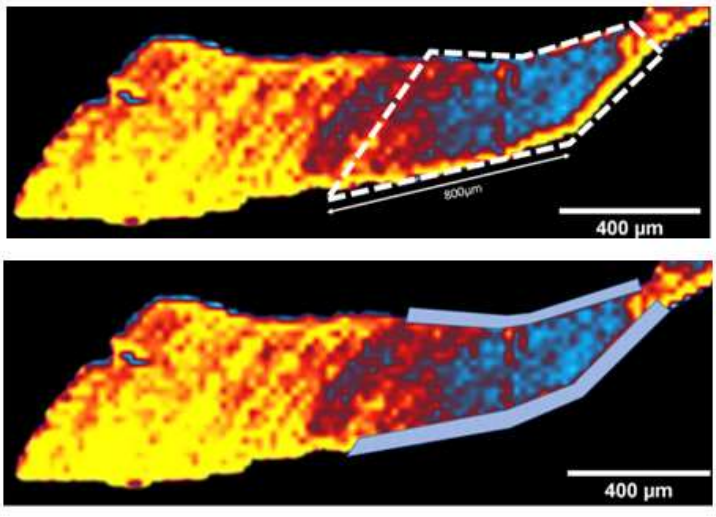

Figure 6.1.5: Pre-treatment of two-dimensional representations of otolith elemental concentration.

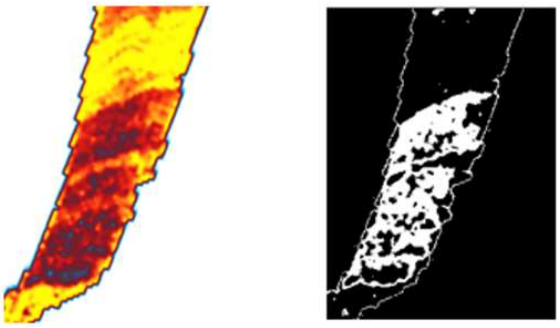

Figure 6.1.6: Example of binarization of elemental concentration to be used as explanatory variables.

Trace element concentration of 10 additional samples of unknown were measured by the LA-ICP-MS and are currently ready for calibration calibrated against international standards. The NN classifier developed under this task will be used to determine the origin of the mixed sample, particularly individuals from Morocco, that were assigned to one population using genetic markers and to the other population using otolith stable isotopes (Brophy et al. 2020).

6.1.4 Conclusions

Two-dimensional mapping of trace elements allows a refined identification of individual bluefin tuna origin, which can serve to answer ecological questions, such as controversies between genetic and otolith stable isotope data. Moreover, two-dimensional mapping of trace elements reveals spatial heterogeneity across the otolith sections allowing to identify fluctuations in specific tracers, such as Sr, Ba and Mn that would not be evident from single transects. The examination of elemental patterns in a two- dimensional scale contribute to a greater appreciation of otolith composition, which translates into increased understanding about stock dynamics, migration patterns or connectivity between habitats of bluefin tuna.

6.2 Task 2: Analyses of carbon and oxygen isotope ration ($\delta^{13}C$ and $\delta^{18}O$) in otolith of bluefin tuna captured in the potential mixing zones

6.2.1 Introduction

Understanding the degree of connectivity between eastern and western populations of Atlantic bluefin tuna is essential for the management of the species. Prior research has shown that stable carbon and oxygen isotopes ($\delta^{13}C$ and $\delta^{18}O$), are valuable for discriminating bluefin tuna from Gulf of Mexico and Mediterranean nurseries (e.g. Rooker et al. 2008). During the previous GBYP phases, otolith $\delta^{13}C$ and $\delta^{18}O$ analyses suggested that western origin contributions were negligible in the Mediterranean Sea, Bay of Biscay and Strait of Gibraltar, but mixing rates could be considerable, in some years, in the central North Atlantic, Canary Islands and western coast of Morocco (Rooker et al. 2014; Fraile et al., 2015,). To further assess and monitor the spatial and temporal variability of mixing proportions throughout the North Atlantic Ocean, a total of 119 otoliths were analyzed for $\delta^{13}C$ and $\delta^{18}O$. The selection included otoliths from the central North Atlantic (N=49) and Norwegian Sea (N=23) captured in 2018 and from the western Moroccan coast captured in 2019 (N=44). This task builds on prior research carried out under the GBYP program, and by increasing the sample size, we aim to better understand interannual variations of mixing rates in the North Atlantic Ocean.

6.2.2 Material and Methods

In this section, we investigate the origin of bluefin tuna collected in the central North Atlantic Ocean (east of the 45ºW management boundary), Norwegian Sea and Moroccan coast using stable $\delta^{13}C$ and $\delta^{18}O$ isotopes in otoliths. Samples utilized for this study (N=116) were collected in 2018 by Japanese longliners operating in the central North Atlantic, by the Norwegian fleet in September 2018, and in the western Moroccan traps in May 2019 (Figure 6.2.1).

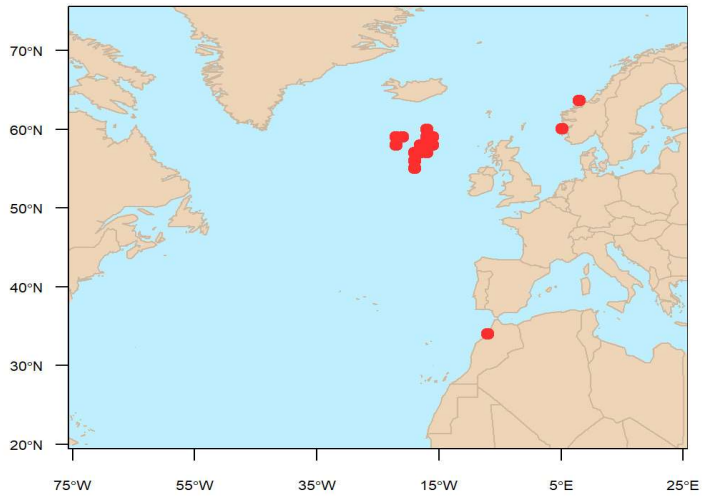

Figure 6.2.1: Sample distribution in the North Atlantic Ocean.

Otolith handling followed the protocols previously described in Rooker et al. (2008). Briefly, following extraction by GBYP participants, sagittal otoliths of bluefin tuna were cleaned of excess tissue with nitric acid (1%) and deionized water. One sagittal otolith from each bluefin tuna specimen was embedded in Struers epoxy resin (EpoFix) and sectioned using a low speed ISOMET saw to obtain 1.5 mm transverse sections that included the core. Following attachment to a sample plate, the portion of the otolith core corresponding to approximately the yearling periods of bluefin tuna was milled from the otolith section using a New Wave Research MicroMill system. A two-vector drill path based upon otolith measurements of several yearling bluefin tuna was created and used as the standard template to isolate core material following Rooker et al. (2008). The pre-programmed drill path was made using a 500 µm diameter drill bit and 15 passes each at a depth of 50 µm was used to obtain core material from the otolith. Powdered core material was transferred to silver capsules and later analyzed for $\delta^{13}C$ and $\delta^{18}O$ on an automated carbonate preparation device (KIEL-III) coupled to a gas-ratio mass spectrometer (Finnigan MAT 252). Stable $\delta^{13}C$ and $\delta^{18}O$ isotopes are reported relative to the PeeDee belemnite (PDB) scale after comparison to an in-house laboratory standard calibrated to PDB.

Stable isotope signals of mixed stocks were compared with yearling samples from Mediterranean and Gulf of Mexico nurseries revised in GBYP-Phase 3 and presented in

Rooker et al. (2014). HISEA software (Millar 1990) was used to generate direct maximum likelihood estimates (MLE) of mixed-stock proportions in each of the mixing zones. HISEA computes the likelihood of fish coming from a nursery area with characterized isotopic signature. MLE estimator is defined as the composition that maximizes the likelihood of the entire mixed fishery sample (Millar 1990). Uncertainty in estimation is addressed by re-sampling the baseline data 500 times with replacement and bootstrapping the mix data (n=1000).

6.2.3 Results and Discussion

$\delta^{13}C$ and $\delta^{18}O$ were measured in the otolith cores of bluefin tuna from the central North Atlantic and compared to baseline populations from the Mediterranean Sea and Gulf of Mexico (Figure 6.2.2).

Otolith $\delta^{18}O$ and $\delta^{13}C$ values corresponded well with those measured in yearling otoliths from the eastern (Mediterranean) and western (Gulf of Mexico) nurseries. Previous otolith chemical analyses indicated that individuals from both production zones readily cross the 45°W management boundary, and mixing of the eastern and western population occurs throughout the North Atlantic Ocean. Mixing proportions were found to be important particularly in the western side of the Atlantic Ocean. Otoliths from the central North Atlantic analyzed during the current phase were captured in the northern geographic region situated east of the 45ºW boundary (Fig. 6.2.1). In 2018, otolith $\delta^{13}C$ and $\delta^{18}O$ values from this region were comprised almost entirely by the eastern (Mediterranean) population (Fig. 6.2.2 central left). To get an overall view of the mixing of the two populations in this region, we combined all the $\delta^{13}C$ and $\delta^{18}O$ measurements performed so far within the GBYP phases (otoliths collected between 2009 and 2018) and compared with baseline values (Fig. 6.2.2 central right). Mixed-stock analyses using Maximum Likelihood Estimates (MLE) indicated that catches in the central North Atlantic were comprised almost exclusively of the Mediterranean population in 2018, and over the time accounted for less than 10% of the sample (Table 6.2.1). Our data suggest that the presence of western migrant is minor, and therefore, Mediterranean population is the main component of Japanese fisheries operating east of the 45ºW management boundary.

Otoliths of ABFT from the Norwegian Sea were found to be connected to the Mediterranean population, based on their $\delta^{13}C$ and $\delta^{18}O$ values. Samples analyzed during the current and previous phases (from 2018 and 2019 respectively) were combined to get

a better representation of the region (Fig. 6.2.2 upper right). Mixing proportions were calculated using the Hisea mixture model, and 100% of the tuna captured in the Norwegian Sea from 2018 to 2019 were assigned to the eastern population. Based on these results, Mediterranean population would be the only contributor to the Norwegian fisheries.

The north-west African coast (Moroccan traps) has been identified as a putative mixing area of eastern and western populations (Rooker et al. 2014). The contribution of western individuals to the east Atlantic fisheries is of particular interest to resource managers because of the strong asymmetrical production between the two populations (Secor, 2015). Based on the stable isotope markers, our results indicate that in 2019, bluefin tuna captured by Moroccan traps were entirely of Mediterranean origin (Fig. 6.2.2 lower left and Table 6.2.1). The combination of all the isotope values analyzed under the GBYP program suggest that the Mediterranean population is the main contributor to Moroccan fisheries, and that the contribution of western migrant in this region is a sporadic phenomenon (Fig. 6.2.2 lower right).

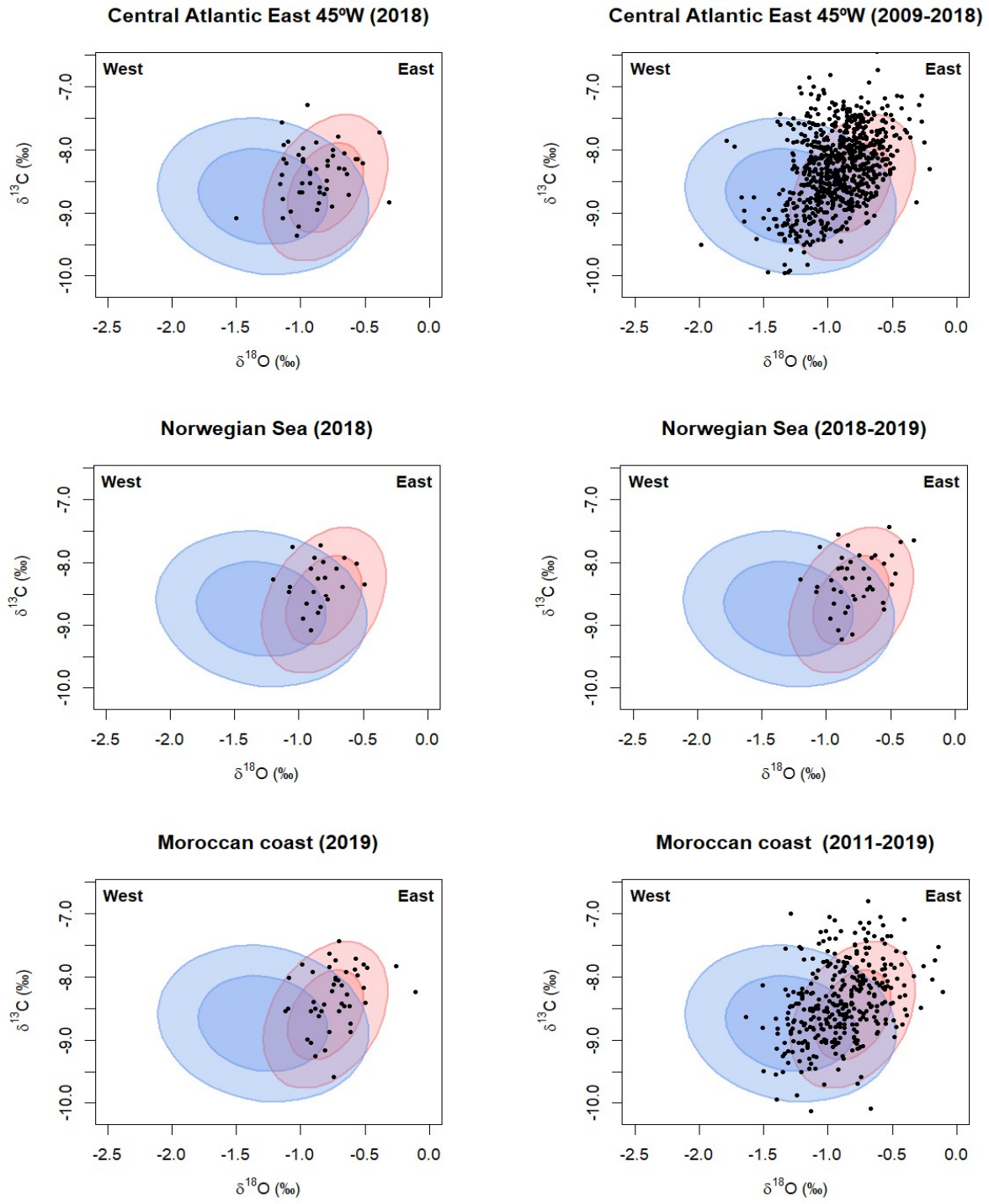

Figure 6.2.2: Confidence ellipses (1 and 2 SD or ca. 68% and 95% of sample) for otolith $\delta^{13}C$ and $\delta^{18}O$ values of yearling bluefin tuna from the east (red) and west (blue) nurseries along with the isotopic values (black) for otolith cores of bluefin tuna of unknown origin collected from three locations during the current GBYP Phase 11 (left) and during previous GBYP Phases (right).

Table 6.2.1: Maximum-likelihood estimates of the origin of bluefin tuna from Norwegian Sea, Central North Atlantic (east of the 45ºW boundary), and Moroccan coast analyzed under the current and previous contracts. Estimates are given as percentages. The mixed-stock analysis (HISEA program) was run under bootstrap mode with 1000 runs to obtain standard deviations around estimated percentages (± %).

Area	Years	West (%)	East (%)	SD	N
Norway	2018	0%	100%	0%	23
	2018-2019	0%	100%	0%	43
Central North Atl. (east of 45ºW)	2018	2%	98%	3%	49
	2009-2018	9%	91%	3%	749
Moroccan coast	2019	0%	100%	2%	47
	2011-2019	6%	94%	3%	396

Otolith $\delta^{13}C$ and $\delta^{18}O$ values were statistically analyzed and individuals were assigned to source populations with associated levels of probability. The identification of individual origin is needed for at least two main reasons: the construction of stock-age-length-keys, and the comparison/improvement of individual assignments based on different types of markers (i.e., genetic, otolith shape and stable isotopes).

Among the classification methods tested with the baseline dataset, it has been shown that Quadratic Discriminant Function Analysis (QDFA) performs the best attaining the highest classification accuracy (Fraile et al. 2015). Thus, QDFA was used to provide posterior probabilities for each pair of $\delta^{13}C$ and $\delta^{18}O$ values. During GBYP Phase-8 it was shown that higher classificatory power was attained by using the adult baseline, composed of spawning adults from the Mediterranean and Gulf of Mexico rather than the classical yearling baseline. Individual probabilities using the adult and yearling baselines (presented in GBYP Phase-8 and Phase-3 respectively) were estimated. Overall, individual assignments by QDFA (using either yearling or adult baseline) yield higher mixing proportions than MLE method in the three regions studied, but considering the confidence intervals around the estimated averages (i.e. mean±2*s.d), the results are generally concordant (Table and Figure 6.2.3). Full posterior probabilities of the bluefin

tuna otoliths analyzed in the current phase have been included in the Appendix 3 of the current report.

Table 6.2.3: *Individual probabilities of eastern and western origin based on Quadratic Discriminant Analysis using Yearling (age-0) and Adult references.*

Area	Years	West (%)	East (%)	Unk (%)	Baseline	N
Norway	2018	4.4	82.6	13	Yearling	23
		4.3	74	21.7	Adult	
Central North Atl. (east of 45ºW)	2018	14.3	63.3	22.4	Yearling	49
		12.2	65.3	22.5	Adult	
Moroccan coast	2019	6.4	83	10.6	Yearling	47
		6.4	78.7	14.9	Adult	

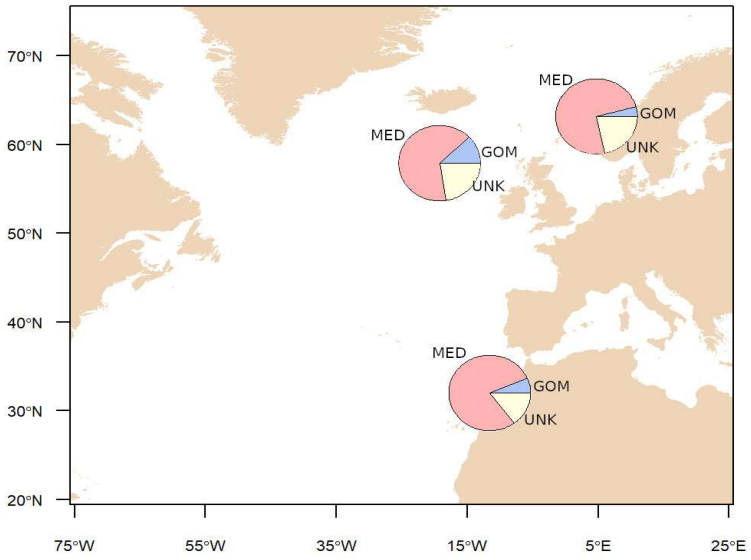

Figure 6.2.3*: Origin of bluefin tuna (Thunnus thynnus) captured in Norwegian Sea, central North Atlantic and Moroccan coast analyzed during GBYP Phase 11. Individual origin assignments are estimated using Quadratic Discriminant Function Analysis with adult spawners as reference samples (Brophy et al. 2020).*

6.2.4 Conclusions

The results from the current phase confirmed that the main contributor of bluefin tuna captured in the eastern side of the Atlantic Ocean, from the Norwegian Sea to central and eastern North Atlantic, is the Mediterranean population. The presence of western migrants was minor in the central North Atlantic and Morocco, accounting for less than 10% of the catches, and was null in the Norwegian Sea.

6.3 Task 3: Further understanding of the relationships between environmental histories of bluefin tuna and otolith microchemistry signals.

6.3.1 Introduction

During phase 9 and 10, considerable progress was made in developing an approach for reconstructing movements of Atlantic bluefin tuna using otolith microchemistry patterns. This task builds on this progress by cross-calibrating the methodologies (IRMS and SIMS) that are used to measure otolith microchemistry, by integrating the information that is provided by different approaches and by building a collection of otoliths for future studies of migration patterns in relation to age and stock origin. In addition, initial steps were taken to establish an experiment in a tuna farm to validate relationships between environmental conditions and otolith oxygen stable isotopes.

6.3.2 Material and Methods

Cross calibration of methodologies

Otolith sections analysed in previous phases using SIMS were re-analysed using IRMS. A total of 29 otoliths were included in the reanalysis. For some otoliths there was insufficient material in the analysed section to produce reliable data from the IRMS analysis; removal of these data left data from 23 otoliths for comparison of IRMS and SIMS measurements (Table 6.3.1)

Table 6.3.1: Numbers of otolith sections from each group analysed using IRMS in phase 11 and by SIMS in phase 10.

Group	Sampling areas	Sample number	Region analysed with IRMS and SIMS
Disputed origin	Eastern Atlantic	3	Core and edge
Disputed origin		2	Core
Young of the year Atlantic	Gibraltar	6	Whole transect
Young of the year Med	Eastern, Western and Central Mediterranean	6	Whole transect
Mediterranean farmed	Central Mediterranean	5	Edge
Mediterranean farmed		1	Core and edge

The 1.5mm thick otolith sections had been previously embedded in epoxy resin, adhered to a 60mm diameter epoxy block and coated with a layer of gold for SIMS analysis. For the IRMS analysis, the otolith portion for analysis (core, edge or whole life history transect) was identified and that portion of the otolith was milled from the otolith section using a New Wave Research MicroMill system. Powdered otolith material was removed using a 300 μm diameter drill bit. To maximise the amount of material available for analysis the section was drilled from the surface all the way through until the resin was reached. Powdered core material was transferred to plastic vials and later analyzed for $\delta^{13}C$ and $\delta^{18}O$ on an automated carbonate preparation device (KIEL-III) coupled to a gas-ratio mass spectrometer (Finnigan MAT 252). Stable $\delta^{18}O$ isotopes are reported relative to the PeeDee belemnite (PDB) scale after comparison to an in-house laboratory standard calibrated to PDB.

For each otolith transect analysed using IRMS, the δ18O measurements from SIMS spots taken along the same transect were averaged (Table 6.3.2) and the two sets of measurements were related to each other using linear regression. The relationship was

compared to a previous calibration equation derived from IRMS and SIMS measurements from Pacific cod (Helser et al., 2018).

The squared residuals from the SIMS/IRMS regression were related to several measures of variability in the mean $\delta^{18}O$ SIMS measurements: the coefficient of variation (CV) of the SIMS measurements for each transect; the length of the transect (transect length); the number of SIMS spots on the transect (spot number); the spatial resolution of the SIMS measurements (spot number/transect length).

Table 6.3.2: Length of otolith transects analysed using IRMS and the number of spots within each transect previously analysed using SIMS

Transect type	Mean transect length (sd)	Mean number of SIMS spots (range)
Whole life history (YoY)	940.0 (151.1)	25 (20-33)
Core	926.7 (144.0)	31 (18-48)
Edge	195.6 (54.6)	7 (3-13)

Otolith samples available for future investigation of migration patterns using SIMS

The ICCAT samples database, maintained by AZTI, was queried to identify otolith samples for future investigation of Atlantic bluefin migration patterns using SIMS analysis. The purpose was to identify: 1) adults (medium and large size classes) from the mixing areas for which two otoliths and age information were available, and for which origin had been determined using genetics; 2) adults collected from the Mediterranean during the spawning season for which two otoliths and age information were available. The future analysis of $\delta^{18}O$ profiles form these samples using SIMS would facilitate a comparison between fish that are known to have undertaken a long-range migration away from the main spawning areas with individuals known to spawn in the Mediterranean.

Validation experiment groundwork

Available models of electronic tag were examined to determine the most suitable for tagging of medium sized Atlantic bluefin of ~60kg and 10 tags were purchased. The design of a future validation experiment on a tuna farm in Malta was discussed with partners in AquaBiotech and IFREMER.

6.3.3 Results and Discussion

Cross calibration of methodologies

Mean $\delta^{18}O$ values from the SIMS transects were linearly related to the IRMS measurements for the same otolith portions (R2 = 0.63, Figure 6.3.1). The relationship was similar to that described for Pacific cod (Helser et al., 2018), although the intercept was higher and the slope was less steep (Figure 6.3.1).

The squared residuals from the regression were not correlated with any of the measures of variability in the SIMS transects.

Due to its high spatial resolution, the SIMS approach more appropriate for reconstructing migration patterns across the life history of individual fish compared to IRMS. However, IRMS is less expensive and time-consuming and is the most appropriate and widely used method for determining nursery ground origin. This cross calibration of the SIMS and IRMS methodologies enables comparison between studies and integration of results to better understand the migration patterns of the western and eastern stocks.

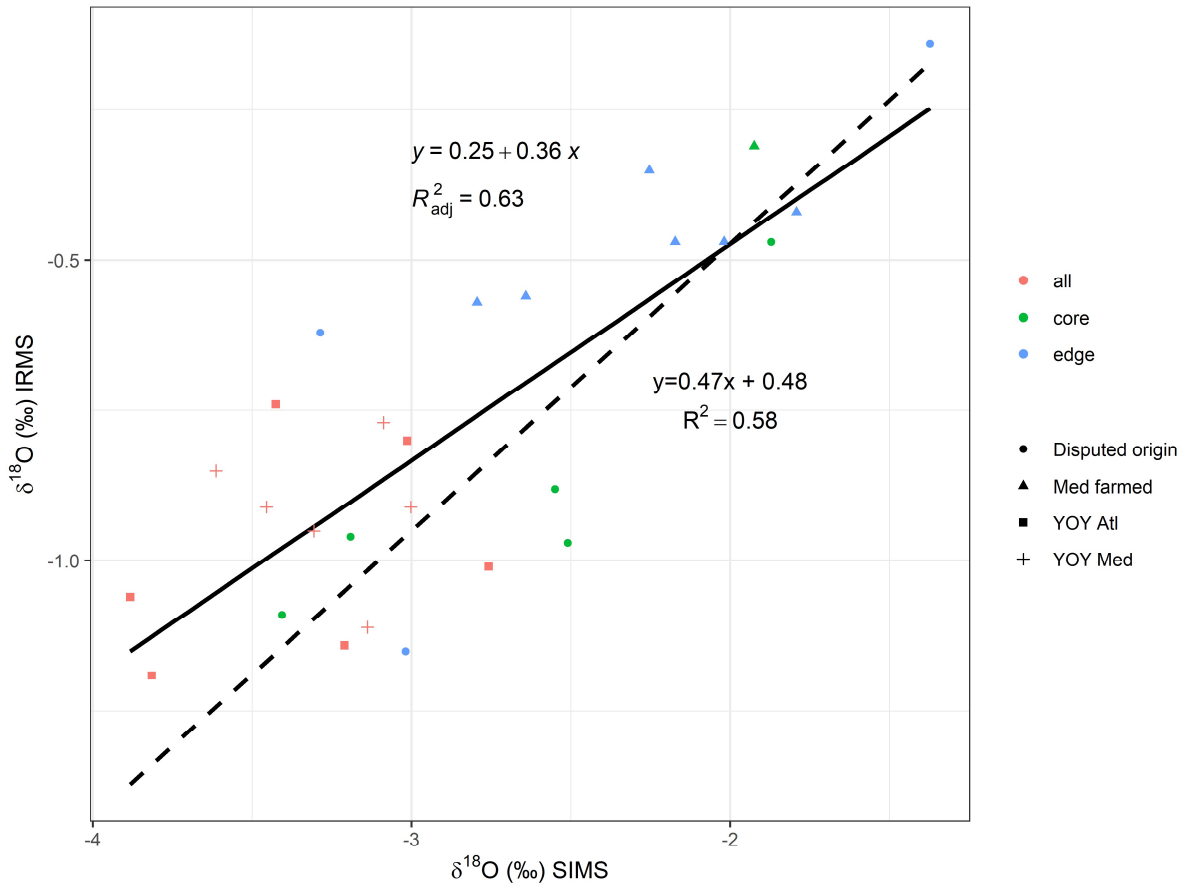

Figure 6.3.1: Plot of the relationship between mean $\delta^{18}O$ values from SIMS transects and the IRMS $\delta^{18}O$ values for the same otolith portions. The solid line is regression line for these data, with the corresponding equation and R2 value shown above it. The dashed line is the regression line from Hesler et al (2018), based on $\delta^{18}O$ SIMS and IRMS data from six Pacific cod otoliths.

Otolith samples available for future investigation of migration patterns using SIMS

A total of 349 adults were identified from the database from which two otoliths were collected, which were aged and for which had been assigned to a stock based on otolith chemistry, genetics or both (Table 6.3.3). These fish were collected in the mixing areas and in the Mediterranean. Future analysis of these otoliths using SIMS could help to establish the age at which Atlantic bluefin begin to undertake wide-range migrations and to identify differences in life history between migratory and resident fish.

Table 6.3.3: Numbers of individuals in the database identified for potential future investigation using SIMS.

Group	Origin	Origin assigned based on	Count
North Atlantic Mixing Areas	Western Atlantic	Genetics and otolith chemistry	6
North Atlantic Mixing Areas	Eastern Atlantic	Genetics and otolith chemistry	170
Eastern Mediterranean	Eastern Atlantic	Otolith chemistry	39
Western Mediterranean	Eastern Atlantic	Otolith chemistry	12
Central Mediterranean	Eastern Atlantic	Otolith chemistry	122

Validation experiment groundwork

Ten TDR-MK9 archival tags were purchased from Wildlife Computers for future deployment within a tuna farm in the Mediterranean. The tags will record internal and ambient temperature and depth and are suitable for deployment on fish down to 50Kg. An opportunity to deploy the tags in a farm in Malta has been identified, through collaboration with AquaBioTech and Ifremer. Experimental pens will be established at this farm for a separate project, so suitable infrastructure and support will be available to complement deployment of these tags. Strontium chloride has been identified as a suitable internal tag for marking the experiment start time in the otolith. Strontium chloride is non-toxic so it's use is compatible with human consumption of the fish; it has been used successfully to mark the otoliths of Pacific bluefin tuna (Clear et al., 2000). Discussions with farm managers regarding protocols and logistics are underway. Animal ethics approval would need to be sought through the Maltese authorities; information regarding this process is being provided by Simeon Degura (AquaBioTech).

Once deployed the tags can provide highly detailed individual environmental histories and internal temperatures that can be paired with $\delta^{18}O$ profiles for the period in captivity to establish relationships between environmental conditions and otolith stable isotopes. Water samples from the farm would provide estimates of the conditions experienced by the group, while data collected using internally implanted archival tags could help to account for between individual variability in otolith microchemistry. As well as

supporting the refinement of a $\delta^{18}O$ fractionation equation, this validation study could allow the time of formation of annual growth bands in the otolith to be established.

6.3.4 Conclusions

The cross calibration of the SIMS and IRMS methodologies established the relationship between $\delta^{18}O$ obtained using the two techniques. The resulting regression can be used to compare data across studies and integrate information from the two approaches.

Otolith material held by AZTI can support future investigation of age-related migration patterns and differences between components of the stock using SIMS analysis of $\delta^{18}O$.

Good progress has been made during this phase to conduct a tagging experiment on Atlantic bluefin tuna held within a farm. This experiment could provide information about the relationship between otolith $\delta^{18}O$ and environmental conditions and the influence of internal physiology on that relationship and could be used to validate the periodicity of annual growth bands in the otolith.

References

Brophy, D, Rodríguez-Ezpeleta, N, Fraile, I and Arrizabalaga, H., 2020. Combining genetic markers with stable isotopes in otoliths reveals complexity in the stock structure of Atlantic bluefin tuna (Thunnus thynnus). Scientific Reports, 10, 14675.

Clear, N.P., Gunn, J.S., Rees, A.J., 2000. Direct validation of annual increments in the otoliths of juvenile southern bluefin tuna, *Thunnus maccoyii*, by means of a large-scale mark-recapture experiment with strontium chloride. Fishery Bulletin 98, 25-40.

Fraile, I., Arrizabalaga, H. and Rooker, J.R., 2015. Origin of Atlantic bluefin tuna (Thunnus thynnus) in the Bay of Biscay. ICES Journal of Marine Science: Journal du Conseil 72: 625-634.

Helser, T.E., Kastelle, C.R., McKay, J.L., Orland, I.J., Kozdon, R., Valley, J.W., 2018. Evaluation of micromilling/conventional isotope ratio mass spectrometry and secondary ion mass spectrometry of δ18O values in fish otoliths for sclerochronology. Rapid Communications in Mass Spectrometry 32, 1781-1790.

Limburg, K. E., Olson, C., Walther, Y., Dale, D., Slomp, C. P., and Høie, H., 2011. Tracking baltic hypoxia and cod migration over millennia with natural tags. Procedings of Natural Academy of Science, U.S.A. 108, 177–182.

Limburg, K. E., Wuenschel, M. J., Hüssy, K., Heimbrand, Y., and Samson, M., 2018. Making the otolith magnesium chemical calendar-clock tick: plausible mechanism and supporting evidence. Review in Fisheries Science and Aquaculture, 26, 479–493.

Millar, R.B., 1990. Comparison of methods for estimating mixed stock fishery composition. Canadian Journal of Fisheries and Aquatic Sciences 47: 2235-2241.

Rodríguez-Ezpeleta, N., Díaz-Arce, N., Walter, J.F., Richardson, D.E., Rooker, J.R. et al. 2019. Determining natal origin for improved management of Atlantic bluefin tuna. Front. Ecol. Environ. 17, 439–444.

Rooker, J. R., H. Arrizabalaga, I. Fraile, D. H. Secor, D. L. Dettman, N. Abid, P. Addis, S. Deguara, F. S. Karakulak, A. Kimoto, O. Sakai, D. Macias, and M. N. Santos. 2014. Crossing the line: migratory and homing behaviors of Atlantic bluefin tuna. Marine Ecology Progress Series 504:265-276.

Rooker, J. R., D. H. Secor, G. De Metrio, R. Schloesser, B. A. Block, and J. D. Neilson. 2008. Natal Homing and Connectivity in Atlantic Bluefin Tuna Populations. Science 322:742-744.

Shiao, J.C., T.F. Yui, H. Høie, U. Ninnemann and S.K. Chang. 2009. Otolith O and C stable isotope composition of southern bluefin tuna *Thunnus maccoyii* (Pisces: Scombridae) as possible environmental and physiological indicators. Zoological Studies 48: 71–82.

7. SORTING BFT LARVAE IN PLANKTON SAMPLES FROM THE BAY OF BISCAY

Task Leader:

María Santos (AZTI)

Participants:

AZTI: Beatriz Beldarrain, Iñaki Rico, Iñigo Onandia

7.1 Introduction

Eastern Atlantic bluefin tuna (ABFT) migrates from the Mediterranean to the Bay of Biscay for feeding (Arrizabalaga et al.2019; Arregui et al.2018). But recently, evidence of bluefin tuna larvae outside the Mediterranean Sea, in the Bay of Biscay, has been reported (Rodriguez et al. 2021). During the previous GBYP phases, samples collected in the Bay of Biscay were analyzed, and one ABFT larvae was found in 2019. During 2021, taking advantage of the ABFT index acoustic survey, specific plankton samples were collected in search of ABFT.

7.2 Material and Methods

7.2.1 Sample collection

Taking into advance the ABFT acoustic survey (BFT Index), on board a commercial vessel in the Bay of Biscay (16-27 June 2021), plankton samples were collected to look for ABFT larvae in this area (ABFT laying period Jun-Jul-Aug). Even if few adult individuals were detected in the area, plankton hauls were carried out, even knowing that the probability of finding an ABFT eggs was going to be low.

The study area in the Bay of Biscay was from 3ºW to the French coast and from the Cantabric coast to 45ºN (Fig. 7.1). The survey was carried out outside the platform (200m depth), were the probability of finding ABFT is usually higher. The plankton sampling was performed at sunset, after the completion of the acoustic transects and fishing

activities for ABFT adults' abundance estimations. The presence of adults was low in most of the areas, so plankton samplings were only performed in 4 stations.

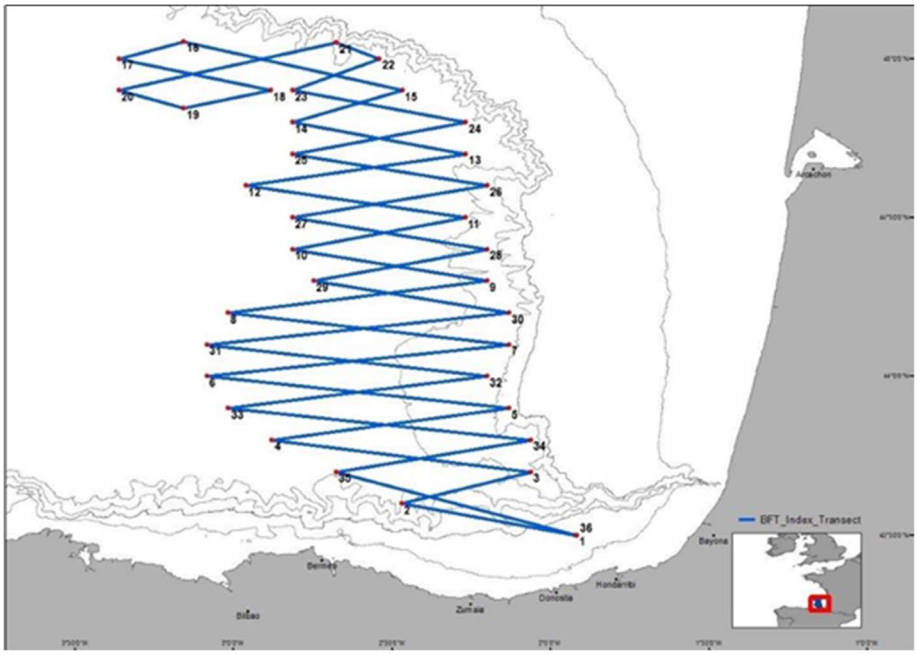

Figure 7.1.: Area of study with the acoustic transects (blue lines) for the adult ABFT abundance index survey.

At each station, an oblique plankton haul was performed using a BONGO60 net with a net mesh size of 250 µm while the vessel was navigating at 2 knots during 20min. The net was lowered to a maximum depth of 30-40m. A 35 kg depressor was used to allow for a correct deployment of the net. "G.O. 2030" flowmeters were used to estimate afterwards the filtered volume. Sampling depth, temperature, salinity, and fluorescence profiles were obtained at each sampling station using a CTD RBR-XR420 coupled to the net.

Immediately after each haul, the net was washed, and the sample obtained was fixed in ethanol 96%.

Table 7.1. Details of larvae sampling at each station

Station	Date	H gm start	H gm end	Lat start	Lon start	Lat end	Lon end	net
1	25/06/2021	19:10	19:35	445721	31065	445783	31082	Bongo60 (250 µm)
2	26/06/2021	12:23	12:50	443939	23310	443920	23340	Bongo60 (250 µm)
3	26/06/2021	20:20	20:50	442400	21200	na	na	Bongo60 (250 µm)
4	27/06/2021	3:35	4:00	432650	15075	43286	15012	Bongo60 (250 µm)

7.2.2 Larvae identification

Larvae species other than clupeids were extracted from the plankton samples under the binocular. ABFT larvae were looked for under a stereoscopic microscope. Visual identification was based on pigmentation patterns, number of myomers, morphologic and meristic characteristics, taking advantage of the last year identification experience and following the descriptions by Alemany (1997), Fahay (2007), Rodriguez et al. (2017), Puncher et al. (2015) and ABFT larvae photos from an incubation experiment carried out in 2012 by AZTI, in the laboratory of IEO Mazarrón-Murcia (Spain) and from a survey carried out in 2012 in the Balearic Sea.

7.3 Results and Discussion

Among the 4 plankton samples obtained, we found no evidence of ABFT larvae (Table 7.2). One larvae of *Sarda sarda* was detected, whose identification was corroborated genetically (Fig.7.2).

Table 7.2. Larvae found in the plankton samples analyzed for ABFT larvae

Station	ABFT lv	*Sarda sarda lv*	*Auxeis rochei lv*	Other lv	Total lv
1	0	0	0	540	541
2	0	0	0	63	63
3	0	0	0	272	272
4	0	1	0	436	437

Two main factors may contribute to explain the lack of bluefin tuna larvae in the sampled area. The first one, the absence of adult bluefin tuna in the area during the survey days, where few juvenile or pre-adult fish were only found. The second one is the limited number of plankton surveys carried out (N=4). More plankton samples are needed to draw further conclusions, ideally covering the entire adult distribution area.

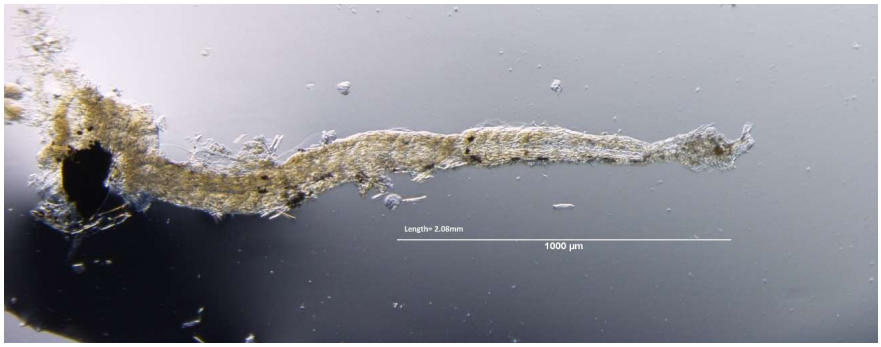

Figure 7.2: Sarda sarda larvae found in station 4 (43º26.50'N 1º50.75' W)

References

Alemany F, Quintanilla L, Velez-Belchi P, Garcia A and others (2010) Characterization of the spawning habitat of Atlantic bluefin tuna and related species in the Balearic Sea (western Mediterranean). Prog Oceanogr 86: 21–38

Arregui, I., Galuardi, B., Goñi, N., Lam, C.H., Fraile, I., Santiago, J., Lutcavage, M. and Arrizabalaga, H. (2018) Movements and geographic distribution of juvenile bluefin tuna in the Northeast Atlantic, described through internal and satellite archival tags. ICES Journal of Marine Science doi:10.1093/icesjms/fsy056.

Arrizabalaga, H., Arregui, I., Medina, A., Rodríguez-Ezpeleta, N., Fromentin, J.-M. and Fraile, I. (2019) Life History and Migrations of Mediterranean Bluefin Tuna In: The Future of Bluefin Tunas: Ecology, Fisheries Management, and Conservation.B. Block (ed.) Johns Hopkins University Press, pp. 67-93.

Corriero A, Desantis S, Deflorio M, Acone F, Bridges CR, De la Serna JM, Megalofonou P, De Metrio G. Histological investigation on the ovarian cycle of the bluefin tuna in the western and central Mediterranean. Journal of Fish Biology. 2003;63(1):108–119. doi: 10.1046/j.1095-8649.2003.00132.x.

Goñi, N., Uranga, J., Arregui, I., Onandia, I., Martinez, U., Boyra, G., Melvin, G.D., Godard, I. and Arrizabalaga, H. (2018) Acoustic-based fishery-independent abundance index of juvenile bluefin tunas in the Bay of Biscay: Results from the first three surveys and challenges. Collect. Vol. Sci. Pap. ICCAT, 76(x): SCRS/2018/145

Karakulak S, Oray I, Corriero A, Deflorio M, Santamaria N, Desantis S, De Metrio G. Evidence of a spawning area for the bluefin tuna (Thunnus thynnus L.) in the eastern Mediterranean. Journal of Applied Ichthyology. 2004;20(4):318–320. doi: 10.1111/j.1439-0426.2004.00561.x

Mackenzie, Brian & Mariani, Patrizio. (2012). Spawning of Bluefin Tuna in the Black Sea: Historical Evidence, Environmental Constraints and Population Plasticity. PloS one. 7. e39998. 10.1371/journal.pone.0039998.

Puncher, G N, Alemany F, Arrizabalaga H, Cariani A and Tinti F. Misidentification of bluefin tuna larvae: a call for caution and taxonomic reform. Rev Fish Biol Fisheries (2015) 25:485–502 DOI 10.1007/s11160-015-9390-1

Reglero P., Ciannelli L., Alvarez-Berastegui D., Balbín R., Lopez-Jurado J.L., Alemany F., (2012) Geographically and environmentally driven spawning distributions of tuna species in the western Mediterranean Sea, Marine ecology progress series, 2012, 463:273-284 pp.

Richardson DE, Marancik KE, Guyon JR, Lutcavage ME, Galuardi B, Lam CH, Walsh HJ, Wildes S, Yates DA, Hare JA. Discovery of a spawning ground reveals diverse migration strategies in Atlantic bluefin tuna (Thunnus thynnus) Proceedings of the National Academy of Sciences of the United States of America. 2016;113(12):3299–3304. doi: 10.1073/pnas.1525636113.

Rodriguez J.M., Johnstone C. and Lozano-Peral D. 2021. Evidence of Atlantic bluefin tuna spawning in the Bay of Biscay, north-eastern Atlantic. Journal of Fish Biology, 99, 964-969.

Rodriguez, J.M., Alemany, F. and Garcia A. 2017. A guide to the eggs and larvae of 100 common Western Mediterranean Sea bony fish species. FAO, Rome, Italy, 256 pp.

Susca V, Corriero A, Deflorio M, Bridges CR, De metrio G. New results on the reproductive biology of bluefin tuna (Thunnus thynnus) in the Mediterranean. ICCAT Collective Volume of Scientific Papers. 2001;52:745–751.

8. SORTING, IDENTIFICATION AND COUNTING OF ATLANTIC BLUEFIN TUNA LARVAE PRESERVED IN ETHANOL 90% FOR GENETICS

Task Leader:

Patricia Reglero (CBBA)

Participants:

CBBA: Nelly Calcina, Asvin Perez, Melissa Martin

8.1 Introduction

The collection of Atlantic bluefin tuna larvae in the main spawning area of the NW Mediterranean Sea provides a novel opportunity to provide samples of the early life stages of this species to the biological sample bank. Adults and juveniles that can be potentially used for further studies including genetics, otolith microchemistry or basic biology have long been sampled in the framework of GBYP. Less effort has been directed towards the early life stages of the species. National programs ensure collecting tuna larvae every summer in the main spawning ground for Bluefin tuna using Bongo nets. One collector is formalin preserved and these samples that are routinely used to identify bluefin tuna larvae since formalin is the best preservation method for the maintenance of pigments used for taxonomic identification and it is further used for the estimation of the larval index used in the assessments. However, preservation in formalin is not suitable for potential uses besides species identification, which would include genetics, otoliths and many other applications. Only since 2019 one of the collectors used in the sampling is preserved in ethanol, the preservation method that ensures larvae can be used for other purposes rather than species identification. This activity is focused in providing larval samples preserved in ethanol to the GBYP so that a number of samples can guarantee in the future further analyses.

This is the main task, to select at least 500 identified bluefin tuna larvae in 30 stations sampled during the oceanographic survey conducted in 2019 in the main tuna spawning ground in the Western Mediterranean.

8.2 Field sampling and laboratory processing

We sorted and identified bluefin tuna fish larvae from 30 stations randomly selected from a cruise that took place around the Balearic Islands, western Mediterranean Sea, during June-July 2019. The larvae were separated and identified from a Bongo net (90-cm diameter and 500-µm mesh size) that was towed obliquely down to 30-m depth for 8-12 minutes at 2 knots cruising speed and preserved directly in 100% ethanol for further processing. The larvae were also separated and identified from a Multinet sampling that was towed at different depths and preserved directly in 100% ethanol for further processing. We used a dissection microscope to identify bluefin tuna larvae and sorted them from the total plankton sample. In addition, the different stages described in the larvae development were identified: yolk sac, preflexion, flexion, or postflexion. The individuals sorted were preserved in 100% ethanol in different 4 ml jarks and kept in the freezer for the perfect conservation.

8.3 Results

We identified 2880 individuals from 30 samples collected during 2019. In 18 samples, bluefin tuna larvae were found and in 12 samples the absence of bluefin tuna larvae was confirmed (Table 8.1).

Table 8.1*: Number of bluefin tuna larvae collected during the TU0619 survey*

Survey	Structure	N° of BFT larvae
TU0619	Multinet	1
TU0619	Multinet	0
TU0619	Multinet	0
TU0619	Multinet	0
TU0619	Multinet	0
TU0619	Multinet	0
TU0619	Multinet	0
TU0619	Multinet	0
TU0619	Multinet	0

TU0619	Bg90	0
TU0619	Bg90	1
TU0619	Bg90	2
TU0619	Bg90	15
TU0619	Bg90	21
TU0619	Bg90	33
TU0619	Bg90	2715
TU0619	Bg90	1
TU0619	Bg90	0
TU0619	Bg90	0
TU0619	Bg90	16
TU0619	Bg90	9
TU0619	Bg90	4
TU0619	Bg90	0
TU0619	Bg90	15
TU0619	Bg90	7
TU0619	Bg90	6
TU0619	Bg90	1
TU0619	Bg90	16

9. ACKNOWLEDGMENT

This work was carried out under the provision of the ICCAT Atlantic Wide Research Programme for Bluefin Tuna (GBYP), funded by the European Union, by several ICCAT CPCs, the ICCAT Secretariat and by other entities (see: https://www.iccat.int/GBYP/en/Overview.asp). The contents of this report do not necessarily reflect the point of view of ICCAT or of the other funders, which have not responsibility about them, neither do them necessarily reflect the views of the funders and in no ways anticipate the Commission's future policy in this area.

10. APPENDICES

Appendix 1: Report f the Epigenetic Ageing (see "AnnexI_reportEpigeneticsAgeing.docx")

Appendix 2: Database as of 31ST MAY 2022 (see "DATABASE_2022_4_ICCAT.xlsx).

Appendix 3: Result of otoliths analyzed under Otolith Microchemistry (see "Annex Table 1")

Annex Table 1: Individual probabilities of being from the western population based on otolith $\delta^{13}C$ and $\delta^{18}O$ using Quadratic Discriminant Analysis Function, using as a reference samples yearlings from the east and west nurseries (YB) and spawning adults (AB).

general ID	Date [dd/mm/yyyy]	Latitude	Longitude	Total Length [cm]	Total Weight [Kg]	prob (0-1) Western QDFA (80%) YB	prob (0-1) Western QDFA (95%) AB
NRIF-CA-L-2978	09/10/2018	59	-22	204	142	0.191	0.205
NRIF-CA-L-2985	14/10/2018	59	-17	217	215	0.088	0.034
NRIF-CA-L-2989	17/10/2018	58	-18	233	263	0.080	0.041
NRIF-CA-L-2995	24/10/2018	55	-19	202	174	0.037	0.012
NRIF-CA-L-3004	08/10/2018	57	-17	206	162	0.144	0.121
NRIF-CA-L-3007	09/10/2018	58	-17	235	220	0.414	0.322
NRIF-CA-L-3010	19/10/2018	57	-17	235	255	0.032	0.008
NRIF-CA-L-3013	20/10/2018	57	-17	228	209	0.136	0.099
NRIF-CA-L-3019	23/10/2018	56	-19	223	197	0.409	0.667
NRIF-CA-L-3025	25/10/2018	56	-19	229	239	0.113	0.079
NRIF-CA-L-3028	29/10/2018	55	-19	212	182	0.138	0.109
NRIF-CA-L-3031	27/09/2018	59	-21	238	268	0.207	0.190
NRIF-CA-L-3034	30/09/2018	59	-22	234	242	0.297	0.338
NRIF-CA-L-3037	02/10/2018	59	-22	224	224	0.205	0.168
NRIF-CA-L-3040	05/10/2018	59	-22	208	157	0.715	0.584
NRIF-CA-L-3043	07/10/2018	59	-22	219	154	0.299	0.233
NRIF-CA-L-3046	09/10/2018	59	-22	222	200	0.205	0.165
NRIF-CA-L-3049	09/10/2018	59	-22	258	360	0.589	0.800
NRIF-CA-L-3052	09/10/2018	59	-22	215	208	0.780	0.683
NRIF-CA-L-3055	12/10/2018	59	-22	245	285	0.396	0.165
NRIF-CA-L-3058	12/10/2018	59	-22	234	246	0.902	0.778
NRIF-CA-L-3061	14/10/2018	58	-22	178	109	0.102	0.065
NRIF-CA-L-3063	14/10/2018	58	-22	227	187	0.149	0.076
NRIF-CA-L-3066	10/10/2018	57	-18	209	162	0.171	0.166
NRIF-CA-L-3069	11/10/2018	57	-17	217	187	0.058	0.024
NRIF-CA-L-3072	13/10/2018	57	-17	219	220	0.716	0.741
NRIF-CA-L-3078	17/10/2018	57	-17	220	201	0.649	0.615
NRIF-CA-L-3081	20/10/2018	57	-18	240	222	0.723	0.677
NRIF-CA-L-3084	23/10/2018	57	-19	199	155	0.466	0.649
NRIF-CA-L-3087	25/10/2018	57	-19	213	187	0.298	0.304
NRIF-CA-L-3090	27/10/2018	57	-19	205	151	0.620	0.752
NRIF-CA-L-3093	02/10/2018	59	-16	211	148	0.061	0.026
NRIF-CA-L-3096	03/10/2018	59	-16	221	202	0.131	0.102
NRIF-CA-L-3099	05/10/2018	59	-16	250	287	0.324	0.218
NRIF-CA-L-3102	06/10/2018	59	-16	226	205	0.376	0.586
NRIF-CA-L-3105	07/10/2018	59	-16	249	253	0.303	0.230
NRIF-CA-L-3108	08/10/2018	59	-16	219	198	0.332	0.386
NRIF-CA-L-3111	10/10/2018	59	-16	233	229	0.710	0.774
NRIF-CA-L-3114	13/10/2018	59	-17	231	227	0.012	0.002
NRIF-CA-L-3117	14/10/2018	59	-17	222	184	0.056	0.023

NRIF-CA-L-3120	15/10/2018	59	-17	206	139	0.034	0.007
NRIF-CA-L-3123	17/10/2018	59	-16	209	155	0.050	0.018
NRIF-CA-L-3126	19/10/2018	59	-17	198	138	0.031	0.008
NRIF-CA-L-3131	01/10/2018	60	-17	230	224	0.052	0.018
NRIF-CA-L-3146	07/10/2018	58	-16	233	226	0.273	0.025
NRIF-CA-L-3152	08/10/2018	58	-17	223	208	0.992	0.998
NRIF-CA-L-3156	09/10/2018	58	-17	203	150	0.083	0.044
NRIF-CA-L-3159	10/10/2018	58	-17	248	269	0.147	0.101
NRIF-CA-L-3167	22/10/2018	56	-19	215	153	0.041	0.014
IMR-NW-L-476	05/09/2018	63.65	7.95	215	196	0.025	0.006
IMR-NW-L-477	05/09/2018	63.65	7.95	182	120	0.162	0.130
IMR-NW-L-479	05/09/2018	63.65	7.95	211	173	0.181	0.115
IMR-NW-L-480	05/09/2018	63.65	7.95	221	192	0.854	0.852
IMR-NW-L-483	05/09/2018	63.65	7.95	222	211	0.032	0.010
IMR-NW-L-484	05/09/2018	63.65	7.95	204	153	0.049	0.019
IMR-NW-L-487	05/09/2018	63.65	7.95	210	179	0.148	0.077
IMR-NW-L-489	05/09/2018	63.65	7.95	210	172	0.160	0.147
IMR-NW-L-492	05/09/2018	63.65	7.95	216	181	0.138	0.113
IMR-NW-L-494	05/09/2018	63.65	7.95	241	244	0.242	0.312
IMR-NW-L-495	05/09/2018	63.65	7.95	202	151	0.119	0.074
IMR-NW-L-496	05/09/2018	63.65	7.95	219	188	0.225	0.232
IMR-NW-L-497	05/09/2018	63.65	7.95	216	182	0.044	0.008
IMR-NW-L-498	05/09/2018	63.65	7.95	200	160	0.088	0.047
IMR-NW-L-499	05/09/2018	63.65	7.95	198	150	0.497	0.501
IMR-NW-L-500	05/09/2018	63.65	7.95	218	191	0.511	0.542
IMR-NW-L-501	05/09/2018	63.65	7.95	210	174	0.055	0.021
IMR-NW-L-503	05/09/2018	63.65	7.95	206	164	0.101	0.042
IMR-NW-L-508	05/09/2018	63.65	7.95	214	176	0.101	0.064
IMR-NW-L-510	05/09/2018	63.65	7.95	217	195	0.594	0.412
IMR-NW-L-512	05/09/2018	63.65	7.95	208	174	0.086	0.041
IMR-NW-L-514	05/09/2018	63.65	7.95	220	199	0.102	0.065
IMR-NW-L-534	24/09/2018	60.08	5.17	293	465	0.278	0.356
INRH-MO-L-347	01/05/2019	34	-5	230	207	0.053	0.021
INRH-MO-L-348	01/05/2019	34	-5	221	185	0.062	0.026
INRH-MO-L-349	01/05/2019	34	-5	230	207	0.070	0.034
INRH-MO-L-350	01/05/2019	34	-5	208	155	0.058	0.020
INRH-MO-L-351	01/05/2019	34	-5	217	175	0.049	0.010
INRH-MO-L-352	01/05/2019	34	-5	226	197	1.000	1.000
INRH-MO-L-353	01/05/2019	34	-5	230	207	0.132	0.004
INRH-MO-L-354	01/05/2019	34	-5	253	273	0.062	0.024
INRH-MO-L-355	01/05/2019	34	-5	221	185	0.017	0.003
INRH-MO-L-356	01/05/2019	34	-5	221	185	0.059	0.025
INRH-MO-L-357	01/05/2019	34	-5	212	164	0.137	0.105
INRH-MO-L-358	01/05/2019	34	-5	226	197	0.243	0.313
INRH-MO-L-359	01/05/2019	34	-5	235	221	0.052	0.020
INRH-MO-L-360	01/05/2019	34	-5	230	207	0.018	0.004
INRH-MO-L-361	01/05/2019	34	-5	208	155	0.383	0.235
INRH-MO-L-362	01/05/2019	34	-5	230	207	0.046	0.016
INRH-MO-L-363	01/05/2019	34	-5	253	273	0.559	0.608
INRH-MO-L-364	01/05/2019	34	-5	221	185	0.163	0.134
INRH-MO-L-365	01/05/2019	34	-5	199	136	1.000	1.000

INRH-MO-L-366	01/05/2019	34	-5	212	164	0.023	0.006
INRH-MO-L-367	01/05/2019	34	-5	221	185	0.068	0.027
INRH-MO-L-368	01/05/2019	34	-5	235	221	0.032	0.010
INRH-MO-L-369	01/05/2019	34	-5	221	185	0.169	0.132
INRH-MO-L-370	01/05/2019	34	-5	230	207	0.147	0.122
INRH-MO-L-371	01/05/2019	34	-5	221	185	0.109	0.071
INRH-MO-L-372	01/05/2019	34	-5	208	155	0.046	0.015
INRH-MO-L-373	01/05/2019	34	-5	199	136	1.000	1.000
INRH-MO-L-374	01/05/2019	34	-5	244	246	0.067	0.024
INRH-MO-L-375	01/05/2019	34	-5	190	119	0.076	0.036
INRH-MO-L-376	01/05/2019	34	-5	230	207	0.645	0.544
INRH-MO-L-377	01/05/2019	34	-5	204	146	0.034	0.010
INRH-MO-L-378	01/05/2019	34	-5	217	175	0.263	0.355
INRH-MO-L-379	01/05/2019	34	-5	235	221	0.606	0.671
INRH-MO-L-380	01/05/2019	34	-5	199	136	0.189	0.106
INRH-MO-L-381	01/05/2019	34	-5	212	164	0.121	0.047
INRH-MO-L-382	01/05/2019	34	-5	217	175	0.017	0.001
INRH-MO-L-383	01/05/2019	34	-5	226	197	0.127	0.094
INRH-MO-L-384	01/05/2019	34	-5	195	128	0.264	0.347
INRH-MO-L-385	01/05/2019	34	-5	181	103	0.092	0.033
INRH-MO-L-386	01/05/2019	34	-5	195	128	0.205	0.208
INRH-MO-L-387	01/05/2019	34	-5	204	146	0.048	0.018
INRH-MO-L-388	01/05/2019	34	-5	217	175	0.030	0.006
INRH-MO-L-389	01/05/2019	34	-5	195	128	0.016	0.003
INRH-MO-L-390	01/05/2019	34	-5	226	197	0.196	0.179
INRH-MO-L-391	01/05/2019	34	-5	199	136	0.024	0.006
INRH-MO-L-392	01/05/2019	34	-5	208	155	0.367	0.361
INRH-MO-L-393	01/05/2019	34	-5	208	155	0.044	0.016